

Development of a Model for Real-Time Tsunami Forecasting: from VTCS to MOST

Vasily Titov¹, Not a Member Utku Kânoğlu², Not a Member
Costas Synolakis^{3 4}, Member, ASCE

ABSTRACT

We describe the development, testing and implementation of a tsunami real-time forecast model, the Method Of Splitting Tsunami (MOST). MOST is now used as an operational forecast model for the National Oceanic and Atmospheric Administration's Tsunami Warning System, and as a tsunami hazard assessment tool in the U.S., and in many countries around the world. Every step in the development of MOST marked new scientific challenges, improvements of technological and computational capabilities, and new demands of the engineering and hazard mitigation communities for applied and benchmark modeling tools for tsunami hazard assessment.

Keywords: tsunami, long wave, tsunami numerical model, MOST, ComMIT, forecasting, early warning.

INTRODUCTION

On 11 March 2011, scientists from the National Oceanic and Atmospheric Administration (NOAA)'s Center for Tsunami Research (NCTR) were concluding a training session on tsunami modeling at the Tanzania Meteorological Agency at Dar es Salaam, using the

¹Researcher, PhD, NOAA/Pacific Marine Environmental Laboratory, 7600 Sand Point Way Northeast, Seattle, WA 98115, United States. E-mail: Vasily.Titov@noaa.gov

²Associate Professor, Department of Engineering Sciences, Middle East Technical University, Universiteler Mahallesi, Dumlupınar Bulvarı, No: 1, Çankaya/Ankara, 06800 Turkey. E-mail: kanoglu@metu.edu.tr

³Professor, Sonny Astani Department of Civil and Environmental Engineering, Viterbi School of Engineering, University of Southern California, 3620 S. Vermont Avenue, KAP 210 Los Angeles, CA 90089-2531, United States. E-mail: costas@usc.edu

⁴Professor, School of Environmental Engineering, Technical University of Crete, Polytechniupoli, Chania 73100 Greece.

20 Method Of Splitting Tsunami (MOST) model, with a web-enabled interface, the Community
21 Interface for Tsunamis (ComMIT) (Titov et al. 2011). During the last day of the training
22 program, when everything was ready for the final evaluation, notification of a fairly strong
23 earthquake off the coast of Japan arrived. Half an hour later, watched in disbelief, the am-
24 plitude as the tsunami at the tsunameter (The Economist 2003) –the instrument also known
25 as tsunamograph or Deep-ocean Assessment and Reporting of Tsunamis (DART)– closest-
26 to-Japan-coast climbing to a never-before-imagined amplitude of nearly 2 m, at a depth of 5
27 km. Inadvertently, the final examination included the real-time forecast of tsunami flooding
28 that was about to occur.

29 This M_w 9.1 earthquake generated a tsunami which devastated Japan’s east coast on
30 11 March 2011, resulting in the costliest known disaster, and the worst damage in Japan’s
31 history since World War II. While Japan suffered the vast majority of the damage and
32 victims from the tsunami, many coastlines around the Pacific, including Chile’s, experienced
33 flooding. The Pacific Tsunami Warning Center (PTWC) assessments, much improved since
34 the 2004 Boxing Day event, were issued timely and appropriately for most of the population
35 at risk in the Pacific, sadly, beyond the near-field impact areas in Japan. Part of the improved
36 U.S. Tsunami Warning System (TWS) was by then the newly-developed tsunami flooding
37 forecast capability based on MOST.

38 This capability was exercised to produce the first-ever forecast of tsunami inundation in
39 Hawai’i, as part of the operational warning capability test. In addition, MOST was also
40 used in different parts of the world to evaluate the Tohoku tsunami impact, beyond the
41 operational responsibilities of the U.S. TWS, as a proof of concept test for the distributed
42 tsunami forecast capability envisioned for the future (Kânoğlu et al. 2015). Scientists in the
43 U.S., New Zealand, Turkey, and Tanzania worked collaboratively using the same source data
44 to produce coordinated and standardized tsunami hazard assessments for this event.

45 MOST has since undergone additional tests to become an operational model for the U.S.
46 Tsunami Warning Centers (TWCs) for tsunami flooding forecasting. We summarize here

47 the experience and process of the development of the operational capabilities in MOST.

48 **EARLY DEVELOPMENT**

49 The original tsunami propagation code that later became the basis of MOST was devel-
50 oped at the Novosibirsk Computing Center of the Siberian Division of the Russian Academy
51 of Sciences (SDRAS) of what was then the Union of Soviet Socialist Republics (USSR)
52 during the years 1984–1989. A novel numerical scheme was applied to solve the nonlinear
53 shallow water-wave (NSW) equations, without artificial viscosity or application of a friction
54 factor (Appendix I). The technique was based on the splitting method, also known as the
55 method of fractional steps, at that time actively being developed by S. K. Godunov’s group
56 in Novosibirsk (Godunov 1973). Dimensional splitting produces two hyperbolic systems,
57 one in each propagation direction, longitudinally and latitudinally, i.e., it creates two two-
58 dimensional (one spatial plus one temporal directions, 1+1D) problem; each problem was
59 then solved with the method of characteristics, with all real and distinct eigenvalues. The
60 characteristic form of the governing equations made the explicit numerical realization of a
61 well-posed boundary-value problem possible, with an efficient numerical scheme, again refer
62 to Appendix I for details.

63 The above numerical model was first presented to the international community during
64 the 14th International Tsunami Symposium in Novosibirsk (31 July–10 August 1989), by
65 the SDRAS (Titov 1989, Titov 1988). This was the start of series of scientific meetings
66 kicking off the “Decade for the Natural Disaster Reduction” (Bernard 1991). At the time,
67 only tsunami propagation results with fully reflective boundaries were presented, and they
68 were benchmarked with an analytical solution. The code was then applied to the 1983 Sea
69 of Japan tsunami, simulating propagation from its inferred source onto the coast, so as to
70 qualitatively compare the distribution of computed offshore amplitudes with measurements
71 along the eastern coastline of Honshu. Another landmark workshop took place at the Marine
72 Science Center of the University of Southern California (USC), at Catalina Island on 15–
73 18 August 1990, where V. V. Titov presented the Novosibirsk Computing Center’s finite-

74 difference three-dimensional (two spatial plus one temporal directions, 2+1D) algorithm (Liu
75 et al. 1991).

76 Further development of the tsunami numerical model occurred at USC during 1992–
77 1997. The focus was adding inundation onto dry land computations, a vexing problem with
78 a moving boundary, for which no adequate mathematical conditions then existed; earlier
79 computations of the climb of a bore on a beach by Hibberd and Peregrine (1979) (HD)
80 used ad-hoc algorithms; pioneering computations by Pedersen and Gjevik (1983) solved a
81 form of the Boussinesq equations using an elegant Lagrangian formulation which allowed
82 a simple boundary condition at the shoreline; (Kim et al. 1983) had opted for a boundary
83 integral (BIEM) solution of Laplace’s equation for water waves. None of these methods were
84 transferable easily then to 2+1D formulations, particularly for non-idealized geometries.

85 To study the 2+1D terminal effects and runup of tsunamis, we started with the develop-
86 ment of the 1+1D model, known then as VTCS–2 (Titov and Synolakis 1995), which solved
87 the NSW equations without using artificial viscosity or friction factors. After testing the dis-
88 persion, absorption and mass conservation characteristics of the numerical scheme, VTCS–2
89 was applied to the canonical problem (a constant depth region connected to a sloping beach)
90 for the solitary wave runup problem investigated by Synolakis (1987), both experimentally
91 and analytically. Titov and Synolakis (1995) applied the model to both nonbreaking and
92 breaking waves, producing excellent agreement with the Synolakis’ laboratory results, both
93 in the time histories of the surface elevations during the evolution of the wave, and for the
94 maximum runup.

95 A distinct feature of the model was that it did not use any artificial viscosity or friction
96 terms. Hibberd and Peregrine (1979) developed the first published algorithm to numerically
97 study the runup of an infinite bore, a very important first step. Synolakis (1986) noted
98 its inadvertent shortcomings, and attempted to improve it, also on an ad-hoc basis. The
99 propagation on dry land involves both runup and rundown, and grid points need to be
100 introduced and removed, as appropriate, or more precisely, as practical in any specific scheme.

101 As discussed by Synolakis (1989), the HD algorithm used a different numerical procedure for
102 the rundown, to avoid the prediction of negative depths, and the entire procedure was not
103 robust, when applied to evolution over composite beaches. The tip of evolving fronts up or
104 down dry lands is fast moving, while the flow depths are very small, a fact whose significance
105 in educating populations at risk not to assume that the waves will move onland with the
106 same speed it does in the surfzone was not appreciated for about a decade later (Synolakis
107 and Bernard 2006, Kânoğlu et al. 2015). In a code without friction, it was and still remains
108 a challenge to develop a robust algorithm, without spurious numerical instabilities rapidly
109 becoming numerical overflows, and contaminating the entire computation.

110 The resulting shoreline algorithm of Titov and Synolakis (1995) was simpler than exist-
111 ing ones at the time for rough slopes (Kobayashi et al. 1987) for the NSW, and, expectedly
112 simpler than the finite-element solution of the Lagrangian form of the 2+1D Boussinesq
113 equations developed by Zelt (1991). A remarkable feature of the algorithm was its ability to
114 model the runup of breaking waves, which are simulated in MOST as bore-like fronts, with-
115 out additional boundary treatments when breaking occurred, only using the finite-difference
116 scheme dissipation of higher frequencies. The explanation is that the NSW equations pre-
117 serve momentum and mass, and are not influenced by details of breaking, a manifestation
118 of G. B. Witham’s bore rule. Titov and Synolakis (1995) commented that “why these
119 simple equations [referring to the depth-averaged shallow water-wave equations] can even
120 model some details of breaking is still quite puzzling.” These observations were recently
121 re-discovered by Couston et al. (2015).

122 VTCS-2 was then extended into 2+1D, hence is name at the time VTCS-3. The split-
123 ting method was used again and the 1+1D runup technique described above was applied
124 virtually unchanged to the two propagation dimensions; Titov (1997) provides a compre-
125 hensive description of the two models. VTCS-3 was then applied to the first large scale
126 2+1D laboratory experiment, the solitary wave propagation around a conical island, which,
127 while planned before it were completed right after by the 1992 Flores tsunami (Yeh et al.

128 1994). This tsunami hit Babi Island, off Flores creating counterintuitive high runup on the
129 backside of the island. In the laboratory incarnation, once solitary waves hit the front side
130 of the island, they split into two waves, moving with their crests nearly perpendicular to the
131 shoreline, propagated around the island and finally collided behind it, creating spectacular
132 interference and counterintuitive high runup, similar to that observed in the field (Liu et al.
133 1995, Briggs et al. 1995, Kânoğlu 1998). Comparisons of VTCS-3 results with the laboratory
134 data not only showed good agreement in front of the island, but also behind it, where the
135 two wave fronts collided, for both time histories of surface elevations and for the maximum
136 runup.

137 The conical island laboratory experiment did not produce measurements on the enhanced
138 runup along the portion of the shoreline shadowed by the island, as observed during the 2010
139 Mentawais tsunami (Hill et al. 2012). The reason was that the experiments with the conical
140 island did not have a sloping beach installed at the end of the wave basin opposite to the
141 wave generator. Additionally, runup was not measured along the absorbing back wall of
142 the basin. This phenomenon of the islands not sheltering the coastlines along mainlands
143 behind them was explored by Stefanakis et al. (2014) using active learning, which involves
144 an emulator based on Gaussian processes to guide the selection of the query points in the
145 parameter space.

146 In the early nineties, both because 2+1D runup could not be evaluated efficiently with ex-
147 isting methods by most non-coastal engineering groups and because bathymetric/topographic
148 data of adequate resolution were not readily available, threshold models (models with a 10 m
149 high reflective vertical wall a certain “threshold” depth) were favored in geophysical studies
150 (Satake 1994, Piatanesi et al. 1996). Titov and Synolakis (1998) applied VTCS-3 with a 5
151 m depth threshold for the 1994 Kuril Islands tsunami, and a hybrid 2+1D offshore, 1+1D
152 near-shore computation for the 1996 Peruvian tsunami, as threshold computations, because
153 no high-resolution bathymetric and topographic data existed to make meaningful calcula-
154 tions. They then applied VTCS-3 to the 1993 Nansei-oki tsunami and calculated the runup

155 around the Okushiri Island, with 50-, 150-, and 450-m grid resolutions, and also used two
156 threshold models with a vertical wall at 10 m and 50 m depths.

157 All these computations were compared with field measurements revealing that the res-
158 olution of available bathymetric and topographic data sets was more critical than the grid
159 resolution, in the reliability of the overall computation. Interpolating from a coarse grid to
160 produce a finer grid improves numerical accuracy and convergence in the specific numerical
161 computation, but may not necessarily improve physical realism. Claiming that a hazard
162 study is accurate up to 10 m, when interpolated geographical data from 100 m grids were
163 used, this is misleading because there may well be sub-grid features in the area under study.
164 Titov and Synolakis (1998) found that a 150-m grid resolution was necessary to qualitatively
165 reproduce the overall runup distribution, but that a 50-m grid was needed to reproduce the
166 extreme runup, as observed. One important conclusion from Titov and Synolakis (1998) was
167 that small bathymetric features affected runup to the first order, a conclusion subsequently
168 shown analytically by Kânoğlu and Synolakis (1998).

169 The canonical problem of solitary wave propagation, the conical island experiment, the
170 Okushiri data and several other datasets eventually became reference benchmarks for testing
171 tsunami models (Synolakis et al. 2008), and were the basis of two benchmarking workshops,
172 see Yeh et al. (1996) and Liu et al. (2008). The VTCS models (and later MOST) was a
173 tsunami code tested with all available problems of laboratory and analytical cases in both
174 workshops.

175 **DEVELOPMENTS TOWARD NOAA'S REAL-TIME FORECAST TOOL**

176 **Before the 2004 Indian Ocean Tsunami**

177 In 1997, MOST was first introduced as the progression of the VTCS numerical techniques
178 as a tsunami forecast tool (Titov and González 1997). The transition was funded by the
179 Defense Advanced Research Projects Agency (DARPA), which had planned to use MOST
180 to develop tsunami hazard mitigation tools for the Pacific Disaster Center (PDC), and then
181 forecast tsunami impact in Hawai'i from potential tsunami sources in the Alaska–Aleutian

182 subduction zone; at the time Hawai'i was widely considered as the most vulnerable locale in
183 the Pacific.

184 The DARPA methodology was the first to use a new type of data, from a newly devel-
185 oped tsunamograph instrument, later called DART. It measured tsunami amplitudes with a
186 bottom pressure recorder (BPR) intereting changes in the static pressure at the ocean floor,
187 triggered by the passing tsunami waves as they propagated over the instrument. DART was
188 developed by NOAA's Pacific Marine Environmental Laboratory (PMEL), and sensitive to
189 about 1-cm high long-waves at 6000-m depth. (González et al. 1998).

190 At first, measurements were not transmitted to NOAA in real time, but were recovered
191 from the BPR after a year-long deployment. MOST used the BPR records of the 1996 An-
192 dreanov tsunami to test the long-distance tsunami propagation simulation capability (Fig.
193 1). The testing checked MOST's accuracy when using spherical earth coordinates, the influ-
194 ence of the Coriolis forces on tsunami propagation, and the sensitivity of the characteristics
195 of tsunamis to earthquake source parameters.

196 The specific finite-difference scheme of MOST exhibits mild numerical dispersion in the
197 computed solution for propagating long waves, in a certain range of parameters. This feature
198 of MOST was used to simulate dispersion during long-distance propagation, without the
199 complexity and computational cost of the dispersive models with explicit dispersion terms
200 (Burwell et al. 2007). The latter identified the optimal grid resolution and parameter set to
201 simulate the linear dispersion model. The effects of dispersion in long-wave propagation are
202 discussed by Zhou et al. (2012), Glimsdal et al. (2013), An and Liu (2014), Løvhold et al.
203 (2015), and Okal and Synolakis (2016), who show that its main effect may be the change in
204 the sequencing between the first and second leading waves.

205 The DARPA study was the foundation of the real-time model forecast capability using
206 tsunamograph recordings, further developed into the pilot version of Short-term Inundation
207 Forecast for Tsunamis (SIFT) as discussed in Titov et al. (2005b). SIFT introduced stan-
208 dardized three levels of telescoping computational grids in MOST, zooming into the forecast

209 coastal location to resolve the coastal area with adequate mesh resolution for accurate in-
210 undation modeling. In SIFT, the inundation grid resolution was < 150 m, and < 50 m,
211 whenever the data and required warning times allowed. Tsunami observation data from the
212 1993 Okushiri Island, 1994 Kuril Islands and 1996 Andreanov Island tsunamis (Titov and
213 Synolakis 1997, Titov et al. 2005b) confirmed these choices and solidified the standard for
214 the inundation model resolution, first suggested by Titov and Synolakis (1997) for useful in-
215 undation predictions. We note that careful tests of convergence are required for any hazard
216 impact projections, and are usually performed by sequentially reducing the step size (con-
217 sistent with the computational fluid dynamics condition), until there are minimal changes
218 in the final results. For example, when studying harbors, a resolution of 5 m or less may be
219 required, depending on the size of coastal structure (Maravelakis et al. 2014).

220 Simulation of tsunami runup in realistic geophysical conditions by an enlarged group of
221 users, especially in locales with large flat coastal areas, prompted the introduction of an
222 artificial friction term to constrain the energy dissipation during flooding, see for example
223 Bernatskiy and Nosov (2012), thus the Manning formulation was introduced in MOST. The
224 proper friction coefficient for specific areas is determined by multiple testing and comparisons
225 with existing inundation measurements (Tang et al. 2009), given that it is this stage where
226 friction can mostly affect predictions.

227 SIFT uses MOST as its core tsunami simulation tool, as described in detail in Titov
228 (2009). A forecast scenario in SIFT consists of a propagation model whose results are
229 then input in separate coastal inundation models, focused on specific portions of coastlines.
230 A propagation scenario consists of a combination of precomputed propagation simulations
231 (referred to as unit sources), derived from minimizing the differences of actual tsunamograph
232 measurements from an initial scenario based on seismic measurements alone. Each unit
233 “source” or “run” is the result of an evolution simulation from a particular tsunami source
234 of $M = 7.5$, which is part of a continuous line of sources, along major known tsunamigenic
235 areas around the world.

236 Over 1700 such propagation runs are stored in NOAA-PMEL's database which describe
237 tsunami propagation offshore, but the actual flooding forecast is produced using a nonlinear
238 inundation model at high resolution. Near-shore tsunami dynamics and flooding are thus
239 estimated through the telescoping grids from the propagation runs of unit sources of ~ 7 km
240 resolution to the inundation model resolution of ~ 50 m.

241 **Post the 2004 Boxing Day Tsunami**

242 The 2004 Indian Ocean tsunami (Geist et al. 2006) killed nearly one quarter million
243 of unwarned coastal residents (most of whom were uninformed of tsunami hazards), and
244 underscored the need for accurate and timely tsunami forecasts. The first simulation of the
245 2004 tsunami using MOST was produced approximately eight hours after the earthquake;
246 it was far from real-time, at the time of the simulation, the tsunami was claiming one of its
247 last victims in South Africa, and it was based on only one measurement from Cocos Island.
248 The forecast only included offshore estimates of tsunami amplitudes (Titov et al. 2005a).
249 Nevertheless, the often pressing nonstop demands for model data for months after the event
250 vividly demonstrated the need for real-time forecasts, not just for the tsunami warning
251 systems, but also for search and rescue operations, emergency relief planning, resources
252 distribution planning and many other unexpected uses. The fact that the eight-hour late
253 simulation (however crude) might have been the only information from ground zero for a
254 catastrophic tsunami had been hugely underestimated.

255 NOAA then decided to start implementing the SIFT inundation forecast capabilities into
256 operational tsunami warning systems, through the realization that forecast information was
257 also important for hazard assessment immediately after an event. MOST became the core
258 component of NOAA's operational forecast system and the next ten years of MOST ad-
259 vancement were focused on increasing robustness, accuracy, and development of site-specific
260 models for the most vulnerable U.S. coastal communities.

261 Developing models that will be run on demand under the pressure of tsunami warning
262 operations is quite different from traditional model development and application in tsunami

263 research. An operational model must provide accurate, robust and rapid results with mini-
264 mal, or better yet, no interaction at all from programmers. These challenging and conflicting
265 requirements are discussed by Tang et al. (2009) for operational tsunami flooding forecasts,
266 and by Kânoğlu and Synolakis (2015) in terms of methodology.

267 Continuous testing of the model capability with all available tsunami data, especially in
268 real-time mode, was a basic aspect of the development process. Tsunami triggering earth-
269 quakes are large scale experiments providing source information and tsunami measurements
270 for testing. Since the first real-time experimental DART detection of the 17 November 2003
271 Rat Island, Alaska tsunami, over 50 tsunamis have been detected by DARTs; most of them
272 occurred during SIFT development. Table 1 lists representative test results of the SIFT ef-
273 fort. This continuous benchmarking possibly makes MOST the most benchmarked tsunami
274 model in existence at the time of writing.

275 The full U.S. array of 39 DARTs was completed in 2008 (Fig. 2); since 2003, there is at
276 least one tsunamograph record for all tsunamis which impacted coastlines. The earthquake
277 location and the DART data provide the necessary information to adequately define the
278 initial sea state and provide input for the high-resolution inundation models to produce the
279 tsunami coastal impact forecast (Titov 2009, Percival et al. 2011). Hence, every tsunami
280 detected by DARTs post 2003 was analyzed using MOST, to determine the possible accuracy
281 of the newly-developed then flooding forecast modules. Most of these tests were performed
282 in real time, before the tide gage records of the arriving-at-the-coast tsunami were available,
283 so as to develop standard operational procedures. A simple metric was used to assess the
284 error of maximum predicted versus measured amplitudes at tide gages, for each observation
285 with a better than 4 to 1 signal-to-noise ratio as follows:

$$286 \quad E_{forecast} = |H_{forecast} - H_{observation}| / H_{observation} \times 100\%. \quad (1)$$

287 Table 1 lists representative events examined and hundreds of real-time forecasts of tsunami

288 time series at coastal sea-level gages. The table summarizes only “true” forecasts that have
289 been completed in real time, before the measurement data had become available. Later as-
290 sessments of each event usually produces better accuracies and includes more comparisons.

291 Obviously, estimates of $E_{forecast}$ depend on the choice of the metric used for the accuracy
292 assessment. $E_{forecast}$ is intentionally oversimplified for comparison purposes, and substantial
293 improvements are possible. For example, our maximum metric ignores the complexity of
294 the forecast of tsunami waves later in the train. NOAA unpublished testing has shown that
295 the leading wave and one or two crests immediately behind it are generally modeled with
296 much higher accuracy than later waves. In some cases, when the largest amplitudes appear
297 several hours after first arrival or more, the underestimate of later amplitudes results in larger
298 overall error, and often the sequencing –which wave carries the largest amplitude in a far-field
299 tsunami– changes, as recently explained by Okal and Synolakis (2016). Nevertheless, the
300 $E_{forecast}$ values illustrate that SIFT provides robust assessments of potential tsunami hazards,
301 and for the larger amplitudes better accuracy, exactly when most needed, i.e. when there is
302 a higher damage potential. Quantitative assessment of the flooding forecast accuracy have
303 been more elusive, because there were no flooding events in the areas where high-resolution
304 forecast models were available. All this changed on 11 March 2011.

305 **The 2011 Tohoku Tsunami**

306 The 11 March 2011 Tohoku tsunami created havoc in Japan and panic throughout the
307 Pacific, testing tsunami preparedness at coastlines around the “Ring of Fire” to their limits.
308 Japan suffered the worst. While very few were killed beyond Japan, all coastlines of the
309 Pacific experienced the tsunami, including waves up to 3-m high and flooding in Chile. The
310 tsunami caused tens of millions of US\$ in monetary losses outside of Japan. The event also
311 created an unprecedented quantity of data to test existing tools and opportunities to develop
312 new ones. The sheer number of observations, the number of witness accounts and especially
313 the amount of instrumental data for this single event rivals the combined amount of tsunami
314 information collected for all prior historical events, dating back to 2000 BC. The wealth of

315 measurements for this event is still being updated, classified and researched.

316 During the Tohoku tsunami, the first real-time operational tsunami flooding forecast
317 was produced. The SIFT forecast system, based on DART data assimilation by MOST was
318 being tested at NOAA’s TWCs on 11 March 2011; however, it was not yet a part of the
319 TWCs’ standard operating procedures. The DART observation system was fully deployed,
320 and 32 site-specific flooding forecast models –most of the planned ones for the Pacific– were
321 already installed at the TWCs for operational testing. The forecast was produced jointly
322 by a test team spread across the world and several time zones, including Seattle, Alaska,
323 Hawai’i and Tanzania, where part of the development team was conducting the United
324 Nations Educational, Scientific and Cultural Organization (UNESCO)–sponsored MOST
325 model training referred to earlier. This exercise was a glimpse of the future distributed
326 tsunami warning and forecast capability envisioned by Bernard et al. (2006). The team
327 produced this pan-Pacific propagation computation, about 90 minutes after the earthquake,
328 right after two DARTs (one U.S.-owned and one Russian-owned) recorded a half-period of
329 the propagating tsunami (Fig. 3), and it became the “authoritative” propagation forecast
330 (the one that fits the tsunamograph measurements best), used widely in further assessments.
331 It was also immediately available to ComMIT users, so they could assess the tsunami threat
332 at different locations around the Pacific (Borrero et al. 2013).

333 The propagation forecast was used as the initial conditions for high-resolution MOST
334 runs for 32 coastal communities in the U.S., producing fast flooding forecast predictions
335 for TWCs’ assessments. The first areas of concern for the U.S. TWCs were the Hawaiian
336 Islands and the West Pacific Territories. Midway Island is one of the closest U.S. territories
337 to the source with estimated tsunami wave arrival 4 h 40 min after the earthquake. At the
338 time, the population of the Midway Atoll National Wildlife Refuge comprised 81 people and
339 hundreds of thousands of protected bird species. The entire population lived on Sand Island
340 with highest elevation of 11 m above sea level. Because of the vulnerability of the location,
341 Midway was one the first sites chosen for the tsunami flooding forecast model. The results

342 showed extensive flooding on both islands of Midway Atoll, but less severe on Sand Island.
343 The residents evacuated to the highest point of the island, which was the third floor of the
344 Charlie Barracks. The information that flooding was expected, but that the wave would
345 not flow over the entire island, was conveyed to the Refuge staff by the TWCs, who thus
346 helped to avoid panic and possible casualties. The flooding forecast was confirmed accurate
347 by both the instrumental measurements from tide gages that were received in real time and
348 by post-event assessments of the flooded area (Fig. 4). The forecast helped the people
349 on the island; however, the animal inhabitants were less fortunate. More than 110,000 of
350 Laysan and black-footed albatross chicks, approximately 22 percent of that year's albatross
351 production, and at least 2,000 adult birds were lost to tsunami flooding on Midway Atoll.

352 The next priority of the U.S. TWCs was the Hawaiian Islands, about three hours of
353 propagation time past the Midway Atoll. The comparisons of the results of the forecast with
354 the measurements from the Midway tide gage increased the confidence in the forecast for
355 Hawai'i. Six of the planned twelve high-resolution inundation models were already developed
356 for Hawai'i and were utilized. The highest amplitudes were predicted for the Kahului harbor
357 with extensive flooding forecasted in the port. No tsunami inundation was predicted for the
358 Honolulu harbor. Evacuation orders were issued for Hawai'i approximately one hour before
359 the arrival of the tsunami, because the practice at the time was to either evacuate all the
360 islands or none. Later, comparisons of the tide gage measurements with predictions at the
361 forecast points vindicated the decision to evacuate. Civil defense surveys taken the following
362 morning confirmed extensive flooding in Kahului, Maui, and elsewhere. Unfortunately, no
363 detailed quantitative measurements of the flooded areas were taken at the time, and most, if
364 not all, potential eyewitnesses were evacuated. Further, critical data to quantify the accuracy
365 of the flooding forecast were lost in the rapid cleanup that followed. There are a few videos
366 documenting the flooding in Kahului, Maui, and in Kona, Hawai'i (aka the Big Island), but
367 they provide only qualitative data and they have yet to be analyzed as in Fritz et al (2012).

368 The MOST forecast predicted tsunami amplitudes over 2 m at several locations along the

369 US West Coast, which were comparable with the Hawai'i tide gage measurements. However,
370 the West Coast was spared from flooding by a significant low tide, which coincided with
371 the time of maximum tsunami wave arrival. While in Hawai'i the tides have a range of
372 approximately 60 cm, many locations along the West Coast experience large tidal variations
373 during the day. The forecast for Crescent City predicted a 2.5 m tsunami, confirmed by the
374 tide gage record (Fig. 5). However, the largest tsunami in the wave train arrived when the
375 tide was 2 m below high water, and mercifully no flooding occurred there or anywhere else
376 along the West Coast. Nevertheless, one person was killed, swept by strong currents and
377 sudden water movements below the high tide mark. Had the tsunami occurred at a different
378 time, Crescent City and other coastal towns might have experienced significant flooding and
379 more lives may have been lost.

380 Even the limited impact of the 2011 Tohoku tsunami along the West Coast demon-
381 strated that including tidal components affected the flooding forecast. NOAA's examination
382 of the forecasting of tide-gage records for several tsunami events indicates that interaction of
383 tsunamis with tides is fairly linear. Coastal sea-level predictions can accurately be obtained
384 by adding tidal components to tide-less tsunami forecasts up to the coastline. The inunda-
385 tion, however, may not be accurately obtained through linear superposition, and has to be
386 computed at changing tide levels. The capability of linearly combining the tidal model to
387 the flooding forecast model input is now being implemented for the next version of opera-
388 tional SIFT. Tsunami currents are suspected to be strongly affected by tides, particularly in
389 ports (Kalligeris et al. , in review), and this requires more careful implementation of tidal
390 prediction into models.

391 In addition to SIFT at NOAA's TWCs, a basin-wide propagation forecast is available for
392 input in MOST inundation models via the Internet-enabled ComMIT interface. ComMIT
393 runs MOST locally, but downloads the initial data from the same database of propagation
394 runs as the operational SIFT system. Thus, forecast scenarios can be used by ComMIT
395 users without interfering with the TWCs operations. During the Tohoku 2011 event, while

396 the tsunami was propagating, ComMIT users produced local forecasts for the same sce-
397 nario. For example, Borrero et al. (2013, 2015a), and Borrero and Goring (2015) produced
398 a MOST forecast and hazard assessment studies for the Tohoku and other tsunamis via
399 ComMIT, providing a real-time prediction of the potential impact at several New Zealand
400 locations, including ports. Their forecasts were later confirmed by comparisons with tide
401 gage measurements.

402 The average accuracy of all 32 forecasts ($E_{forecast}$), when compared with the maximum
403 amplitudes at the tide gages, was approximately 70% (Table 1). The gages measuring
404 amplitudes greater than 1 m exhibited 74% accuracy, and those measuring amplitudes greater
405 than 1.5 m were predicted with 87% accuracy, confirming that locations of potential flooding
406 can be robustly forecasted.

407 Advancing the distributed forecast concept further, NOAA developed a prototype web
408 tool, Tweb, which allows sharing forecast results created with ComMIT, for different coast-
409 lines, via a graphical web client (Bernard and Titov 2015). The tool is now being tested by
410 NOAA as an operational forecast dissemination tool.

411 **Implementation as a NOAA Operational Capability**

412 Making these flooding forecast tools operational at the NOAA's TWCs required more
413 than the one real-time test in 2011. Operational testing and evaluation (OT&E) was con-
414 ducted to ensure robustness and to develop standard operating procedures for using SIFT
415 and its tsunami flooding forecast models in TWCs operations. The Tohoku tsunami data
416 was one of four sets of event data used by TWCs staff to test the tool, which also included
417 data from the 2007 Kuril Islands, 2009 Samoa, and 2010 Chile tsunamis (Fig. 6). During the
418 course of nearly two years of testing, four more tsunamis occurred that were also *naturally*
419 included in the operational tests. In 2013, after almost two years of unprecedented OT&E
420 at TWCs, the first-ever real-time forecast capability based on MOST became operational in
421 August 2013.

422 This testing during the 2011 tsunami was one big step toward the goal referred to as the

423 *the holy grail* by the tsunami science community, i.e., accurately predicting tsunami flood-
424 ing, before the tsunami arrives at any coastline. Efforts of the entire tsunami community for
425 several decades contributed to the creation of a forecast-capable computer code. Scientific
426 standards and benchmarks, laboratory data, computer science developments, engineering
427 and operational implementation of the DART system and many other scientific and engi-
428 neering milestones had to be achieved before MOST was able to produce its operational
429 flooding forecast during the Tohoku event.

430 **WORLDWIDE APPLICATION OF MOST**

431 MOST has been applied in tsunami hazard studies around the world (Rossetto et al.
432 2011). Its first “public” demonstration was during the 24th International Tsunami Sympo-
433 sium (14–16 July 2009) (Satake et al. 2011a, 2011b), for the real-time assessment of the 15
434 July 2009 Fierland, New Zealand tsunami by Uslu et al. (2011). Over 100 tsunami scientists
435 (including personnel from several TWCs) at the Akademgorodok Science Center of SDRAS
436 in Novosibirsk watched the fortuitous show of NOAA personnel producing a inundation
437 forecast right there and projected on the conference room screen. By serendibity, this was
438 the same room where the discussions for the development of inundation models took place
439 twenty years earlier (See the “EarlyDevelopment” section).

440 A similar concept as the SIFT database and real-time forecast of NOAA, but using a
441 different approach, is employed by the Joint Australian Tsunami Warning Centre (JATWC)
442 at the Bureau of Meteorology, Australia. Rather than employing unit sources, JATWC uses
443 earthquakes with magnitudes of 7.5, 8, 8.4, and 9 at specified locations. It then employs
444 a propagation database, prepared with MOST. Comparisons of predictions from the two
445 scenario databases for the 3 May 2006 Tonga and 12 September 2007 Sumatra events are
446 provided in Greenslade and Titov (2008). The same kind of database is in the process of
447 development for the Mediterranean (Kânoğlu et al. 2012).

448 VTCS models and its later version, MOST, have been used in several PhD theses (Bor-
449 rero 2002, Barberopoulou 2006, Uslu 2008, Kalligeris 2016). MOST was also used in support

450 of fundamental research studies such as to identify landslide dislocation sources from earth-
451 quake generated sources considering shoreline runup distribution (Okal and Synolakis 2004),
452 to recover seismic moments from tsunameter records (Okal and Titov 2007), investigating
453 satellite altimetry usage for improved early detection and warning (Hamlington et al. 2012),
454 focusing phenomena observed from N-wave type initial wave displacement (Kânoğlu et al.
455 2013) and sequencing of tsunami –later waves in the train becoming higher than the leading
456 one– (Okal and Synolakis 2016).

457 Several historical events have been investigated with MOST to confirm chronicled and
458 eyewitness accounts gathered in field surveys through interviews with survivors. Examples
459 include the modeling that followed the post-event surveys of the 1 April 1946 Aleutian
460 tsunami in the far-field (Okal et al. 2002) and in the near-field (Okal et al. 2003), the
461 9 July 1956 Amorgos, Greece, tsunami (Okal et al. 2009), the tsunami earthquake of 22
462 June 1932 in Manzanillo, Mexico (Okal and Borrero 2011), the 9 February 1948 tsunami off
463 Karpathos, Greece (Ebeling et al. 2012), and the Dwarskersbos, South Africa, 27 August
464 1969 meteotsunami (Okal et al. 2014).

465 MOST has been extensively used in hazard studies on the U.S. West Coast, especially for
466 the development of inundation maps for California (Borrero et al. 2001, 2004, Barberopoulou
467 et al. 2009, 2011), for Crescent City, California (Uslu et al. 2007, Dengler et al. 2008),
468 for probabilistic tsunami hazard analyses (Uslu 2008), for the probabilistic tsunami hazard
469 assessment for Seaside, Oregon (González et al. 2009), for hazards assessment resulting from
470 harbor modifications (Dengler and Uslu 2011); and the real time (Tang et al. 2012) and
471 hindcast (Wei et al. 2013) studies for the 11 March 2011 Japan tsunami.

472 In terms of worldwide application, other than the studies discussed earlier in the context
473 of validation for the 12 July 1993 Okushiri, 4 October 1994 Kuril Islands, and 21 February
474 1996 Peru events, the 12 July 1998 Papua New Guinea (Synolakis et al. 2002, Lynett et al.
475 2003), the 2004 Boxing Day (Titov et al. 2005a), the 17 July 2006 Java (Fritz et al. 2007), the
476 15 August 2007 Peru (Wei et al. 2008), and the studies of the 29 September 2009 Samoa (Okal

477 et al. 2010, Fritz et al. 2011, Zhou et al. 2012) tsunamis were also performed using MOST.
478 Hazard studies with MOST include tsunamis from possible future earthquakes off Sumatra
479 (Borrero et al. 2006), regional earthquakes off Peru (Okal et al. 2006), other megathrusts in
480 the Indian Ocean (Okal and Synolakis 2008), sources in the South China Sea (Okal et al.
481 2011), in the Mediterranean (Mitsoudis et al. 2012, Valle et al. 2014, England et al. 2015),
482 and unpublished studies in North Africa, the Caribbean and the Gulf of Mexico.

483 **CONCLUSIONS**

484 MOST has been a useful tool for real-time tsunami forecasts and warnings and for applied
485 hazard mitigation. We can draw a few conclusions, helpful in understanding the impact of
486 numerical modeling in coastal engineering.

- 487 1. During the development of MOST, there was extensive testing using laboratory, an-
488 alytical and field data. Titov and Synolakis (1998) tested VTCS-3 with the conical
489 island experiments and confirmed that the code could model the enhanced runup on
490 the lee side of the island. They then used measurements from the 1993 Hokkaido-
491 Nansei-Oki, 1994 Kuril Islands, and 1996 Peru tsunamis, cases which presented sub-
492 stantial computational challenges, such as extreme > 30 m runup, overland flows
493 over a peninsula, and flows over sandbars into lagoons and beyond. In every compu-
494 tational methodology, particularly when moving fluid fronts are involved, there are
495 always unimagined issues and details, necessitating further refinements and conver-
496 gence checks. Continuous testing of numerical methods in geophysical fluid mechanics
497 with measurements from past events is the only proven way for developing reliable
498 practices.
- 499 2. MOST was developed through extensive research efforts, migrating from a 1+1D
500 propagation to a 2+1D propagation, from Cartesian to geophysical coordinates, from
501 a variable grid to telescoping grids, from a frictionless code to one that includes
502 a friction factor. Every transition was tested and results compared with archived

503 versions of earlier codes and benchmarks, to ensure that there were no inadvertent
504 programming errors introduced as source files were edited for improvement. Further,
505 the gradual transitioning allowed for evaluating the impact of the coding additions on
506 the final results, especially since the changes were introduced one at a time. Conver-
507 gence was checked at every stage. While similar evolution may appear impractical,
508 it still remains unwise to develop numerical procedures from scratch, without first
509 understanding the solution of simpler idealized problems.

- 510 3. The source code was disseminated only through special training sessions, often or-
511 ganized by UNESCO, sometimes through individual collaborative work, via specific
512 agreements. Nevertheless, MOST became one of the most used tsunami code in re-
513 search (Rueben et al. 2011, Løvhold et al. 2013). The open source distribution model
514 was not employed for MOST for several reasons. One was to ensure quality control.
515 MOST is an operational code, and tsunami warnings are held to a higher standards
516 with very specific requirements, different from goals of research-focused hazard stud-
517 ies which produce consultancy reports and journal papers. To ensure such quality
518 control with an open-source distribution model requires substantial resources have
519 yet to become available. Besides, there are several excellent “free” BT and NSW
520 codes available for (See Brocchini (2013) for a review of BT models.). Their outputs
521 may differ slightly, for the same initial conditions; however, these differences dwarf the
522 uncertainties in source characterization, or the differences in results when convergence
523 is not checked, or results obtained by inexperienced users.

524 The minimum “training” requirement for MOST were established to avoid situa-
525 tions when high-end tsunami inundation codes are used improperly to forecast future
526 flooding disasters and to make important policy implications that may cost people’s
527 lives. It is not untypical to wonder while reading such studies how convergence of the
528 computations was checked, or even how the grid sizing was determined, since the hy-
529 drodynamic models are often treated as an off-the-shelf black box, without references

530 to original publications and with limited or no tests by community-wide accepted
531 benchmarks.

- 532 4. The developers of MOST had substantial personal experience in tsunami field sur-
533 veys. Field surveys often reveal previously unidentified flow patterns. The longshore
534 variation of runup observed in the 1992 Nicaraguan event, the enhanced runup on the
535 lee side of Babi island in 1992, and along the west coast of the Mentawai Islands in
536 2010 in regions sheltered by smaller offshore islands, and the first tsunami hydrograph
537 measured by field teams in Kessenuma in 2011 (Fritz et al. 2012) are good examples.
538 Further, tsunami survey teams interview eyewitnesses. Their testimonies can lead
539 to paradigm changes, such as the existence of leading depression N-waves first docu-
540 mented in Nicaragua in 1992 (Tadepalli and Synolakis 1994). Surveys not only provide
541 outreach possibilities to educate populations at risk, at a critical time immediately
542 after a disaster, when locals are most interested in extreme natural phenomena, but
543 also provide geophysical context to the visiting scientists.

544 In this regard, applied hazard studies must be considered in a fairly broad context,
545 and include the author’s personal field experiences, particularly in the interpretation of the
546 results. Someone who has not walked on flooded lands, mused over differences in inundation
547 between adjacent beaches, debated why a single structure was left standing while all others
548 were flattened, debated whether a debris-mark on a surviving tree was from the tsunami or
549 carried by the wind, listened to sometimes widely different eyewitness accounts for the same
550 location, or wondered if an overland sediment blanket is consistent with the tsunami that
551 just happened, likely cannot fully interpret a historic report, understand what differences
552 changes in grid resolution can make, or ultimately put flooding predictions in the proper
553 context. As Synolakis and Kânoğlu (2015) argued, what doomed the Fukushima nuclear
554 power plant was the sub-standard pre-disaster coastal engineering study, which not only
555 did not use appropriate design earthquakes, and there was apparently no tsunami-specific
556 field experience among the Tokyo Electric Power Company (TEPCO) engineers to put their

557 flooding predictions in the proper historic and societal context.

558 Predicting the future evolution of coastal engineering is futile and any such attempt will
559 border science fiction. Two decades ago, reliable real-time flooding forecasts were imagined,
560 but no one believed them possible in the near future, but it happened. The immediate
561 next step is the development of timely nearfield warnings, available in 10 min or less after
562 the earthquake ends, as robust as the farfield warnings, which are now very much “under
563 control” (Okal 2015). Preliminary tests of the near-field flooding forecast capability using
564 the 2011 Tohoku data (Fig. 3) and 2015 Chile tsunami forecast (Tang et al. 2016) already
565 show promising results. MOST will further evolve in response of these new goals, and
566 developments under way improve numerical efficiency with parallelization, implement more
567 robust boundary conditions, include more modular structure to allow for faster and more
568 accurate forecasts. There are no immediate plans for MOST to become a full 3-D hydro
569 code, or even add implicit dispersion terms –there are many excellent codes that already
570 have these capabilities. We have little doubt that MOST will continue to be part of the
571 world’s defense against tsunamis, as undoubtedly will other excellent computational codes.

572 We envision that within a decade, real-time flooding forecasts will be possible, within
573 ten minutes or less after an event. We look forward to better documentation to determine
574 if dispersion, compressibility, and stratification are important in flooding forecasts, and to
575 better understanding breaking wave interactions and large scale coherent structures in ports
576 (Borrero et al. 2015b). The plan is to develop design tsunami hydrographs for every tsunami
577 shelter in the world (Fritz et al. 2012, Kânoğlu et al. 2015). We also look forward to
578 standardized training of scientists and engineers, performing tsunami hazard studies and the
579 regulators or consultants who review them.

580 In all tsunami engineering endeavors and developments, we caution scientists and engi-
581 neers to carefully ponder Albert Einstein’s dictum, “everything should be made as simple as
582 possible, but not simpler.”

APPENDIX I. MATHEMATICAL FORMULATION

The 2+1D NSW equations are

$$\begin{aligned}
 h_t + (uh)_x + (vh)_y &= 0, \\
 u_t + uu_x + vu_y + gh_x &= gd_x, \\
 v_t + uv_x + vv_y + gh_y &= gd_y,
 \end{aligned} \tag{2}$$

where $h = \eta(x, y, t) + d(x, y, t)$, $\eta(x, y, t)$ is the amplitude, $d(x, y, t)$ is the undisturbed water depth, $u(x, y, t)$ and $v(x, y, t)$ are the depth-averaged velocities in the x - and y -directions, respectively, and g is the acceleration of gravity. The model does not include a bottom friction term. A variety of boundary and initial conditions can be specified to solve the NSW equations. In general, tsunami generation caused by instantaneous bottom displacements, i.e., $d_0(x, y, t = 0)$, which could be evaluated through Okada's (1992) formulation, is applied at the sea surface.

The splitting method reduces the numerical solution of the 2+1D problem into consecutive solutions of two 1+1D problems:

$$\begin{aligned}
 h_t + (uh)_x &= 0, & h_t + (vh)_y &= 0, \\
 u_t + uu_x + gh_x &= gd_x, & \text{and} & & v_t + vv_y + gh_y &= gd_y, \\
 v_t + uv_x &= 0, & & & u_t + vu_y &= 0.
 \end{aligned} \tag{3}$$

Each of the hyperbolic quasi-linear systems has all real and distinct eigenvalues and can be written in characteristic form as follows:

$$p_1 + \lambda_1 p_x = gd_x, \quad q_1 + \lambda_2 q_x = gd_x, \quad v' + \lambda_3 v' = 0, \tag{4}$$

where the Riemann invariants of this system are as follows:

$$p = u + 2\sqrt{gh}, \quad q = u - 2\sqrt{gh}, \quad v' = v, \tag{5}$$

596 and the three distinct eigenvalues are

$$597 \quad \lambda_1 = u + \sqrt{gh}, \quad \lambda_2 = u - 2\sqrt{gh}, \quad \lambda_3 = u. \quad (6)$$

598 These characteristics are given in the x -direction and could be applied in the y -direction in a
 599 similar manner. Refer to Titov (1997) and Titov and Synolakis (1998) for the details of the
 600 application of the boundary conditions and the finite difference scheme to solve the system.

Note also that the 2+1D NSW equations in spherical coordinates are as follows:

$$\begin{aligned} h_t + \frac{(uh)_\psi}{R \cos \varphi} + \frac{(vh \cos \varphi)_\varphi}{R \cos \varphi} &= 0, \\ u_t + \frac{uu_\psi}{R \cos \varphi} + \frac{vu_\varphi}{R} + \frac{gh_\psi}{R \cos \varphi} &= \frac{gd_\psi}{R \cos \varphi} + \frac{uv \tan \varphi}{R} + f v, \\ v_t + \frac{uv_\psi}{R \cos \varphi} + \frac{vv_\varphi}{R} + \frac{gh_\varphi}{R} &= \frac{gd_\varphi}{R} - \frac{u^2 \tan \varphi}{R} - f u, \end{aligned} \quad (7)$$

where ψ is longitude, φ is latitude, $h = h(\psi, \varphi, t) + d(\psi, \varphi, t)$, $h(\psi, \varphi, t)$ is the amplitude, $d(\psi, \varphi, t)$ is the undisturbed water depth, $u(\psi, \varphi, t)$ and $v(\psi, \varphi, t)$ are the depth-averaged velocities in the longitude and latitude directions respectively, g is the gravity acceleration, f is the Coriolis parameter ($f = 2\omega \sin \varphi$), R is the Earth's radius and ω is the angular velocity of the Earth. For computations, the equations are split into the following two 1+1D systems, as before. The two terms of the momentum equations, $uv \tan \varphi / R$ and $u^2 \tan \varphi / R$, are usually omitted for computations due to smallness, to increase simulation speed.

$$\begin{aligned} h_t + \frac{(uh)_\psi}{R \cos \varphi} &= 0, & h_t + \frac{(vh \cos \varphi)_\varphi}{R \cos \varphi} &= 0, \\ u_t + \frac{uu_\psi}{R \cos \varphi} + \frac{gh_\psi}{R \cos \varphi} &= \frac{gd_\psi}{R \cos \varphi}, & \text{and} & & v_t + \frac{vv_\varphi}{R} + \frac{gh_\varphi}{R} &= \frac{gd_\varphi}{R}, \\ v_t + \frac{uv_\psi}{R \cos \varphi} &= 0, & u_t + \frac{vu_\varphi}{R} &= 0. \end{aligned} \quad (8)$$

601 **ACKNOWLEDGMENTS**

602 This manuscript was partially supported by the project ASTARTE (Assessment, STrat-
603 egy And Risk Reduction for Tsunamis in Europe) Grant 603839, 7th FP (ENV.2013.6.4-3
604 ENV.2013.6.4-3) to the Technical University of Crete and the Middle East Technical Univer-
605 sity (METU). CES also acknowledges the US-National Science Foundation award CMMI-
606 1538624. This study was partially funded by the NOAA's Pacific Marine Environmental
607 Laboratory (PMEL) contribution no. 4383.

NOTATION

The following symbols are used in this paper:

d = undisturbed water depth;

d_0 = initial sea surface (seafloor) displacement;

f = Coriolis parameter;

g = acceleration of gravity;

h = total height of the water column measured from bottom (flow depth);

p, q, v' = Riemann invariants;

R = Earth's radius;

t = time;

u = horizontal component of depth-averaged velocity in x -direction (longitudinal);

v = horizontal component of depth-averaged velocity in y -direction (latitudinal);

η = amplitude;

λ = eigenvalue;

φ = latitude;

ψ = longitude.

REFERENCES

- An, C. and Liu, P. L.-F. (2014). “Characteristics of leading tsunami waves generated in three recent tsunami events.” *Journal of Earthquake and Tsunami*, 08(03), 1440001.
- Barberopoulou, A. (2006). “Investigating the damage potential of seismic seiches: A case study of the Puget Lowland.” Ph.D. thesis, University of Washington, Seattle, Washington.
- Barberopoulou, A., Borrero, J. C., Uslu, B., Kalligeris, N., Goltz, J. D., Wilson, R. I., and Synolakis, C. E. (2009). “New maps of California to improve tsunami preparedness.” *EOS Transactions American Geophysical Union*, 90(16), 137–138.
- Barberopoulou, A., Borrero, J. C., Uslu, B., Legg, M. R., and Synolakis, C. E. (2011). “A second generation of tsunami inundation maps for the state of california.” *Pure and Applied Geophysics*, 168(11), 2133–2146.
- Bernard, E. and Titov, V. V. (2015). “The evolution of tsunami warning systems and products.” *Philosophical Transactions of the Royal Society A: Mathematical, Physical & Engineering Sciences*, 373(2053), 20140371.
- Bernard, E. N. (1991). “Fourteenth International Tsunami Symposium: Opening address.” *Natural Hazards*, 4, 115–117.
- Bernard, E. N., Mofjeld, H. O., Titov, V., Synolakis, C. E., and González, F. I. (2006). “Tsunami: scientific frontiers mitigation, forecasting and policy implications.” *Philosophical Transactions of the Royal Society A-Mathematical Physical and Engineering Sciences*, 364(1845), 1989–2006 Discussion Meeting on Extreme Natural Hazards, Royal Soc, London, England, 26–27 October, 2005.
- Bernatskiy, A. V. and Nosov, M. A. (2012). “The role of bottom friction in models of non-breaking tsunami wave runup on the shore.” *Izvestiya Atmospheric and Oceanic Physics*, 48(4), 427–431.
- Borrero, J. (2002). “Analysis of tsunami hazards in Southern California.” Ph.D. thesis, University of Southern California, Los Angeles, California (August).
- Borrero, J. C., Bell, R., Csato, C., DeLange, W., Goring, D., Dougal Greer, S., Pickett,

638 V., and Power, W. (2013). “Observations, effects and real time assessment of the March
639 11, 2011 Tohoku-oki tsunami in New Zealand.” *Pure and Applied Geophysics*, 170(6-8),
640 1229–1248.

641 Borrero, J. C., Dolan, J. F., and Synolakis, C. E. (2001). “Tsunamis within the eastern
642 Santa Barbara Channel.” *Geophysical Research Letters*, 28(4), 643–646.

643 Borrero, J. C. and Goring, D. G. (2015). “South American tsunamis in Lyttelton Harbor,
644 New Zealand.” *Pure and Applied Geophysics*, 172(3-4), 757–772.

645 Borrero, J. C., Goring, D. G., Greer, S. D., and Power, W. L. (2015a). “Far-field tsunami
646 hazard in New Zealand ports.” *Pure and Applied Geophysics*, 172(3-4), 731–756.

647 Borrero, J. C., Legg, M. R., and Synolakis, C. E. (2004). “Tsunami sources in the southern
648 California bight.” *Geophysical Research Letters*, 31(13), L13211.

649 Borrero, J. C., Lynett, P. J., and Kalligeris, N. (2015b). “Tsunami currents in ports.” *Philo-*
650 *sophical Transactions of the Royal Society A: Mathematical, Physical & Engineering Sci-*
651 *ences*, 373(2053), 20140372.

652 Borrero, J. C., Sieh, K., Chlieh, M., and Synolakis, C. E. (2006). “Tsunami inundation
653 modeling for western Sumatra.” *Proceedings of the National Academy of Sciences of the*
654 *United States of America*, 103(52), 19673–19677.

655 Briggs, M. J., Synolakis, C. E., Harkins, G. S., and Green, D. R. (1995). “Laboratory
656 experiments of tsunami runup on a circular island.” *Pure and Applied Geophysics*, 144(3-
657 4), 569–593.

658 Brocchini, M. (2013). “A reasoned overview on Boussinesq-type models: the interplay
659 between physics, mathematics and numerics.” *Proceedings of the Royal Society A-*
660 *Mathematical Physical and Engineering Sciences*, 469(2160), 20130496.

661 Burwell, D., Tolkova, E., and Chawla, A. (2007). “Diffusion and dispersion characterization
662 of a numerical tsunami model.” *Ocean Modelling*, 19(1-2), 10–30.

663 Couston, L.-A., Mei, C. C., and Alam, M.-R. (2015). “Landslide tsunamis in lakes.” *Journal*
664 *of Fluid Mechanics*, 772, 784–804.

- 665 Dengler, L. and Uslu, B. (2011). “Effects of harbor modification on Crescent City, California’s
666 tsunami vulnerability.” *Pure And Applied Geophysics*, 168(6-7), 1175–1185.
- 667 Dengler, L. A., Uslu, B., Barberopoulou, A., Borrero, J. C., and Synolakis, C. (2008). “The
668 vulnerability of Crescent City, California, to tsunamis generated by earthquakes in the
669 Kuril Islands region of the Northwestern Pacific.” *Seismological Research Letters*, 79(5),
670 608–619.
- 671 Ebeling, C. W., Okal, E. A., Kalligeris, N., and Synolakis, C. E. (2012). “Modern seis-
672 mological reassessment and tsunami simulation of historical hellenic arc earthquakes.”
673 *Tectonophysics*, 530-531, 225–239.
- 674 England, P., Howell, A., Jackson, J., and Synolakis, C. (2015). “Palaeotsunamis and tsunami
675 hazards in the Eastern Mediterranean.” *Philosophical Transactions of the Royal Society
676 A: Mathematical, Physical & Engineering Sciences*, 373(2053), 20140374.
- 677 Fritz, H. M., Borrero, J. C., Synolakis, C. E., Okal, E. A., Weiss, R., Titov, V. V., Jaffe,
678 B. E., Foteinis, S., Lynett, P. J., Chan, I.-C., and Liu, P. L.-F. (2011). “Insights on
679 the 2009 South Pacific Tsunami in Samoa and Tonga from field surveys and numerical
680 simulations.” *Earth-Science Reviews*, 107(1-2, SI), 66–75.
- 681 Fritz, H. M., Kongko, W., Moore, A., McAdoo, B., Goff, J., Harbitz, C., Uslu, B., Kalligeris,
682 N., Suteja, D., Kalsum, K., Titov, V., Gusman, A., Latief, H., Santoso, E., Sujoko, S.,
683 Djulkarnaen, D., Sunendar, H., and Synolakis, C. (2007). “Extreme runup from the 17
684 July 2006 Java tsunami.” *Geophysical Research Letters*, 34(12), L12602.
- 685 Fritz, H. M., Phillips, D. A., Okayasu, A., Shimozono, T., Liu, H., Mohammed, F., Skanavis,
686 V., Synolakis, C. E., and Takahashi, T. (2012). “The 2011 Japan tsunami current veloc-
687 ity measurements from survivor videos at Kesennuma Bay using LiDAR.” *Geophysical
688 Research Letters*, 39(7), L00G23.
- 689 Geist, E. L., Titov, V. V., and Synolakis, C. E. (2006). “Tsunami: Wave of change.” *Scientific
690 American*, 294(1), 56–63.
- 691 Glimsdal, S., Pedersen, G. K., Harbitz, C. B., and Løvhold, F. (2013). “Dispersion of

692 tsunamis: does it really matter?." *Natural Hazards and Earth System Sciences*, 13(6),
693 1507–1526.

694 Godunov, S. K. (1973). *Finite-difference schemes*. Nauka, Moscow, USSR.

695 González, F. I., Geist, E. L., Jaffe, B., Kânoğlu, U., Mofjeld, H., Synolakis, C. E., Titov,
696 V. V., Arcas, D., Bellomo, D., Carlton, D., Horning, T., Johnson, J., Newman, J., Parsons,
697 T., Peters, R., Peterson, C., Priest, G., Venturato, A., Weber, J., Wong, F., and Yalciner,
698 A. (2009). "Probabilistic tsunami hazard assessment at Seaside, Oregon, for near- and
699 far-field seismic sources." *Journal of Geophysical Research-Oceans*, 114, C11023.

700 González, F. I., Milburn, H. M., Bernard, E. N., and Newman, J. C. (1998). "Deep-ocean
701 Assessment and Reporting of Tsunamis (DART): Brief overview and status report." Pro-
702 ceedings of the International Workshop on Tsunami Disaster Mitigation, 19-22 January
703 1998, Tokyo, Japan.

704 Greenslade, D. J. M. and Titov, V. V. (2008). "A comparison study of two numerical tsunami
705 forecasting systems." *Pure and Applied Geophysics*, 165(11-12), 1991–2001.

706 Hamlington, B. D., Leben, R. R., Godin, O. A., Gica, E., Titov, V. V., Haines, B. J., and
707 Desai, S. D. (2012). "Could satellite altimetry have improved early detection and warning
708 of the 2011 Tohoku Tsunami?." *Geophysical Research Letters*, 39, L15605.

709 Hibberd, S. and Peregrine, D. H. (1979). "Surf and run-up on a beach - Uniform bore."
710 *Journal of Fluid Mechanics*, 95, 323–345.

711 Hill, E. M., Borrero, J. C., Huang, Z., Qiu, Q., Banerjee, P., Natawidjaja, D. H., Elosegui,
712 P., Fritz, H. M., Suwargadi, B. W., Pranantyo, I. R., Li, L., Macpherson, K. A., Skanavis,
713 V., Synolakis, C. E., and Sieh, K. (2012). "The 2010 M_w 7.8 Mentawai earthquake: Very
714 shallow source of a rare tsunami earthquake determined from tsunami field survey and
715 near-field GPS data." *Journal of Geophysical Research-Solid Earth*, 117, B06402.

716 Kalligeris, N. (2016). "Large scale coherent structures in ports and other tsunami phenom-
717 ena." Ph.D. thesis, University of Southern California, Los Angeles, California.

718 Kalligeris, N., Skanavis, V., Tavakkol, S., Ayca, A., El Safty, H., Lynett, P. J., and Synolakis,

719 C. E. “Vorticity in a nano-tsunami.” *Geophysical Research Letters* In review.

720 Kânoğlu, U. (1998). “The runup of long waves around piecewise linear bathymetries.” Ph.D.
721 thesis, University of Southern California, Los Angeles, California (August).

722 Kânoğlu, U., Hoto, O., Kalligeris, N., Flouri, E., Aydin, B., Moore, C., and Synolakis, C.
723 (2012). “Tsunami propagation database for the Mediterranean and Aegean Seas.” Abstract
724 NH33A- 1666 presented at 2012, Fall Meeting, AGU, San Francisco, CA, December 3-7.

725 Kânoğlu, U. and Synolakis, C. E. (1998). “Long wave runup on piecewise linear topogra-
726 phies.” *Journal of Fluid Mechanics*, 374, 1–28.

727 Kânoğlu, U. and Synolakis, C. E. (2015). *Tsunami dynamics, forecasting, and mitigation*.
728 Chapter 2 in Hazards and Disasters Series: Coastal and Marine Hazards, Risks, and
729 Disasters, Series Ed. John F. Shroder; volume Eds. Jean T. Ellis and Douglas J. Sherman,
730 Elsevier, pp. 15–57.

731 Kânoğlu, U., Titov, V., Bernard, E., and Synolakis, C. E. (2015). “Tsunamis: bridging sci-
732 ence, engineering and society.” *Philosophical Transactions of the Royal Society A: Math-*
733 *ematical, Physical & Engineering Sciences*, 373(2053), 20140379.

734 Kânoğlu, U., Titov, V. V., Aydin, B., Moore, C., Stefanakis, T. S., Zhou, H., Spillane,
735 M., and Synolakis, C. E. (2013). “Focusing of long waves with finite crest over constant
736 depth.” *Proceedings of the Royal Society A-Mathematical Physical and Engineering Sci-*
737 *ences*, 469(2153), 20130015.

738 Kim, S. K., Liu, P. L.-F., and Liggett, J. A. (1983). “Boundary Integral-Equation solutions
739 for solitary wave generation, propagation and run-up.” *Coastal Engineering*, 7(4), 299–317.

740 Kobayashi, N., Otta, A. K., and Roy, I. (1987). “Wave reflection and run-up rough slopes.”
741 *Journal of Waterway Port Coastal and Ocean Engineering-ASCE*, 113(3), 282–298.

742 Liu, P. L.-F., Cho, Y. S., Briggs, M. J., Kânoğlu, U., and Synolakis, C. E. (1995). “Runup
743 of solitary waves on a circular island.” *Journal of Fluid Mechanics*, 302, 259–285.

744 Liu, P. L.-F., Synolakis, C. E., and Yeh, H. H. (1991). “Report on the International Workshop
745 on long-wave run-up.” *Journal of Fluid Mechanics*, 229, 675–688.

746 P. L.-F. Liu, H. Yeh, and C. Synolakis, eds. (2008). *Advanced numerical models for simulating*
747 *tsunami waves and runup*, Vol. 10 of *Advances in Coastal and Ocean Engineering*. World
748 Scientific Publishing Co. Pte. Ltd., Singapore.

749 Løvhold, F., Lynett, P. J., and Pedersen, G. (2013). “Simulating run-up on steep slopes with
750 operational Boussinesq models; capabilities, spurious effects and instabilities.” *Nonlinear*
751 *Processes in Geophysics*, 20(3), 379–395.

752 Løvhold, F., Pedersen, G., Harbitz, C., Glimsdal, S., and Kim, J. (2015). “Landslide induced
753 tsunamis - a review.” *Philosophical Transactions of the Royal Society A: Mathematical,*
754 *Physical & Engineering Sciences*, 373(2053), 20140376.

755 Lynett, P. J., Borrero, J. C., Liu, P. L.-F., and Synolakis, C. E. (2003). “Field survey and
756 numerical simulations: A review of the 1998 Papua New Guinea tsunami.” *Pure and*
757 *Applied Geophysics*, 160(10-11), 2119–2146.

758 Maravelakis, N., Kalligeris, N., Lynett, P. J., Skanavis, V., and Synolakis, C. E. (2014). “A
759 study of wave amplification in the Venetian harbor in Chania, Greece.” Proceedings of the
760 International Conference on Coastal Engineering, Seoul, June 15 - 20, 2014.

761 Mitsoudis, D., Flouri, E., Chrysoulakis, N., Kamarianakis, Y., Okal, E., and Synolakis, C.
762 (2012). “Tsunami hazard in the southeast Aegean Sea.” *Coastal Engineering*, 60, 136–148.

763 Okada, Y. (1992). “Internal deformation due to shear and tensile faults in a half-space.”
764 *Bulletin of the Seismological Society of America*, 82(2), 1018–1040.

765 Okal, E. A. (2015). “The Quest for Wisdom: Lessons from the 2004-2013 tsunamis.” *Philo-*
766 *sophical Transactions of the Royal Society A: Mathematical, Physical & Engineering Sci-*
767 *ences*, 373(2053), 20140370.

768 Okal, E. A. and Borrero, J. C. (2011). “The ‘tsunami earthquake’ of 1932 June 22 in Man-
769 zanillo, Mexico: seismological study and tsunami simulations.” *Geophysical Journal In-*
770 *ternational*, 187(3), 1443–1459.

771 Okal, E. A., Borrero, J. C., and Synolakis, C. E. (2006). “Evaluation of tsunami risk from
772 regional earthquakes at Pisco, Peru.” *Bulletin of the Seismological Society of America*, 96,

773 1634–1648.

774 Okal, E. A., Fritz, H. M., Synolakis, C. E., Borrero, J. C., Weiss, R., Lynett, P. J., Titov,
775 V. V., Foteinis, S., Jaffe, B. E., Liu, P. L.-F., and Chan, I. C. (2010). “Field Survey of the
776 Samoa Tsunami of 29 September 2009.” *Seismological Research Letters*, 81(4), 577–591.

777 Okal, E. A., Plafker, G., Synolakis, C. E., and Borrero, J. C. (2003). “Near-field survey of
778 the 1946 Aleutian Tsunami on Unimak and Sanak Islands.” *Bulletin of the Seismological
779 Society of America*, 93(3), 1226–1234.

780 Okal, E. A. and Synolakis, C. E. (2004). “Source discriminants for near-field tsunamis.”
781 *Geophysical Journal International*, 158(3), 899–912.

782 Okal, E. A. and Synolakis, C. E. (2008). “Far-field tsunami hazard from mega-thrust earth-
783 quakes in the Indian Ocean.” *Geophysical Journal International*, 172(3), 995–1015.

784 Okal, E. A. and Synolakis, C. E. (2016). “Sequencing of tsunami waves: why the first wave
785 is not always the largest.” *Geophysical Journal International*, 204(2), 719–735.

786 Okal, E. A., Synolakis, C. E., Fryer, G. J., Heinrich, P., Borrero, J. C., Ruscher, C., Arcas,
787 D., Guille, G., and Rousseau, D. (2002). “A field survey of the 1946 Aleutian tsunami in
788 the far field.” *Seismological Research Letters*, 73(4), 490–503.

789 Okal, E. A., Synolakis, C. E., and Kalligeris, N. (2011). “Tsunami simulations for regional
790 sources in the south china and adjoining seas.” *Pure and Applied Geophysics*, 168(6-7),
791 1153–1173.

792 Okal, E. A., Synolakis, C. E., Uslu, B., Kalligeris, N., and Voukouvalas, E. (2009). “The
793 1956 earthquake and tsunami in Amorgos, Greece.” *Geophysical Journal International*,
794 178(3), 1533–1554.

795 Okal, E. A. and Titov, V. V. (2007). “M-TSU: Recovering seismic moments from tsunameter
796 records.” *Pure and Applied Geophysics*, 164(2-3), 355–378.

797 Okal, E. A., Visser, J. N. J., and de Beer, C. H. (2014). “The dwarskersbos, south africa
798 local tsunami of august 27, 1969: field survey and simulation as a meteorological event.”
799 *Natural Hazards*, 74(1), 251–268.

800 Pedersen, G. and Gjevik, B. (1983). “Run-up of solitary waves.” *Journal of Fluid Mechanics*,
801 135, 283–299.

802 Percival, D. B., Denbo, D. W., Eble, M. C., Gica, E., Mofjeld, H. O., Spillane, M. C., Tang,
803 L., and Titov, V. V. (2011). “Extraction of tsunami source coefficients via inversion of
804 DART (R) buoy data.” *Natural Hazards*, 58(1), 567–590.

805 Piatanesi, A., Tinti, S., and Gavagni, I. (1996). “The slip distribution of the 1992 Nicaragua
806 Earthquake from tsunami run-up data.” *Geophysical Research Letters*, 23(1), 37–40.

807 Rossetto, T., Allsop, W., Charvet, I., and Robinson, D. I. (2011). “Physical modelling of
808 tsunami using a new pneumatic wave generator.” *Coastal Engineering*, 58(6), 517–527.

809 Rueben, M., Holman, R., Cox, D., Shin, S., Killian, J., and Stanley, J. (2011). “Optical
810 measurements of tsunami inundation through an urban waterfront modeled in a large-
811 scale laboratory basin.” *Coastal Engineering*, 58(3), 229–238.

812 Satake, K. (1994). “Mechanism of the 1992 nicaragua tsunami earthquake.” *Geophysical*
813 *Research Letters*, 21(23), 2519–2522.

814 Satake, K., Rabinovich, A., Kânoğlu, U., and Tinti, S. (2011a). “Introduction to “Tsunamis
815 in the World Ocean: Past, present, and future. Volume I”.” *Pure and Applied Geophysics*,
816 168(6-7), 963–968.

817 Satake, K., Rabinovich, A., Kânoğlu, U., and Tinti, S. (2011b). “Introduction to “Tsunamis
818 in the World Ocean: Past, present, and future. Volume II”.” *Pure and Applied Geophysics*,
819 168(11), 1913–1917.

820 Stefanakis, T. S., Contal, E., Vayatis, N., Dias, F., and Synolakis, C. E. (2014). “Can small
821 islands protect nearby coasts from tsunamis? An active experimental design approach.”
822 *Proceedings of the Royal Society A-Mathematical Physical and Engineering*, 470(2172),
823 20140575.

824 Synolakis, C. (1986). “The runup of long waves.” Ph.D. thesis, California Institute of Tech-
825 nology, Engineering and Applied Science, Pasadena, California (January).

826 Synolakis, C. and Kânoğlu, U. (2015). “The Fukushima accident was preventable.” *Philo-*

827 *sophical Transactions of the Royal Society A: Mathematical, Physical & Engineering Sci-*
828 *ences*, 373(2053), 20140379.

829 Synolakis, C. E. (1987). “The runup of solitary waves.” *Journal of Fluid Mechanics*, 185,
830 523–545.

831 Synolakis, C. E. (1989). “Wave reflection and run-up on rough slopes - Discussion.” *Journal*
832 *of Waterway, Port, Coastal and Ocean Engineering-ASCE*, 115(1), 139–143.

833 Synolakis, C. E., Bardet, J. P., Borrero, J. C., Davies, H. L., Okal, E. A., Silver, E. A.,
834 Sweet, S., and Tappin, D. R. (2002). “The slump origin of the 1998 Papua New Guinea
835 Tsunami.” *Proceedings of the Royal Society A-Mathematical Physical and Engineering*
836 *Sciences*, 458(2020), 763–789.

837 Synolakis, C. E. and Bernard, E. N. (2006). “Tsunami science before and beyond Boxing Day
838 2004.” *Philosophical Transactions of the Royal Society A-Mathematical Physical and Engi-*
839 *neering Sciences*, 364(1845), 2231–2265 Discussion Meeting on Extreme Natural Hazards,
840 Royal Soc, London, England, 26–27 October, 2005.

841 Synolakis, C. E., Bernard, E. N., Titov, V. V., Kânoğlu, U., and González, F. I. (2008).
842 “Validation and verification of tsunami numerical models.” *Pure and Applied Geophysics*,
843 165(11-12), 2197–2228.

844 Tadepalli, S. and Synolakis, C. E. (1994). “The run-up of N-waves on sloping beaches.”
845 *Proceedings of the Royal Society-Mathematical and Physical Sciences*, 445(1923), 99–112.

846 Tang, L., Titov, V. V., Bernard, E. N., Wei, Y., Chamberlin, C. D., Newman, J. C., Mofjeld,
847 H. O., Arcas, D., Eble, M. C., Moore, C., Uslu, B., Pells, C., Spillane, M., Wright, L., and
848 Gica, E. (2012). “Direct energy estimation of the 2011 Japan tsunami using deep-ocean
849 pressure measurements.” *Journal of Geophysical Research-Oceans*, 117, C08008.

850 Tang, L., Titov, V. V., and Chamberlin, C. D. (2009). “Development, testing, and appli-
851 cations of site-specific tsunami inundation models for real-time forecasting.” *Journal of*
852 *Geophysical Research-Oceans*, 114, C12025.

853 Tang, L., Titov, V. V., Moore, C., and Wei, Y. (2016). “Real-time assessment of the 16

854 September 2015 Chile tsunami and implications for near-field forecast.” *Pure and Applied*
855 *Geophysics*, 173, 369–387.

856 The Economist (2003). “Tsunamis: The next big wave. Science and Technology. 14 August
857 2003. Last accessed on 10 August 2015 at <http://www.economist.com/node/1989485>.

858 Titov, V. (1997). “Numerical modeling of long wave runup.” Ph.D. thesis, University of
859 Southern California, Los Angeles, California (May).

860 Titov, V., Rabinovich, A. B., Mofjeld, H. O., Thomson, R. E., and González, F. I. (2005a).
861 “The global reach of the 26 December 2004 Sumatra tsunami.” *Science*, 309(5743), 2045–
862 2048.

863 Titov, V. and Synolakis, C. (1997). “Extreme inundation flows during the Hokkaido-Nansei-
864 Oki tsunami.” *Geophysical Research Letters*, 24(11), 1315–1318.

865 Titov, V. V. (1988). “Numerical model of tsunami accounting for the wave shoaling.” *Report*
866 *No. Preprint, 771*, Novosibirsk, VC SOAN USSR (In Russian).

867 Titov, V. V. (1989). “Numerical modeling of tsunami propagation by using variable grid.”
868 Proceedings of the IUGG/IOC International Tsunami Symposium, Novosibirsk, USSR,
869 46–51.

870 Titov, V. V. (2009). *Tsunami forecasting*. In the Sea, Ideas and Observations on Progress in
871 the Study of the Seas; Volume 15 Tsunamis, Chapter 12. Bernard, EN and Robinson, AR
872 (Eds.). Harvard University Press, Cambridge, MA. 371–400.

873 Titov, V. V. and González, F. I. (1997). “Implementation and testing of the Method of
874 Splitting Tsunami (MOST) model.” *Report No. Technical Memorandum ERL PMEL-112*,
875 NOAA/Pacific Marine Environmental Laboratory. 11pp.

876 Titov, V. V., Gonzalez, F. I., Bernard, E. N., Eble, M. C., Mofjeld, H. O., Newman, J. C.,
877 and Venturato, A. J. (2005b). “Real-time tsunami forecasting: Challenges and solutions.”
878 *Natural Hazards*, 35(1), 41–58.

879 Titov, V. V., Moore, C. W., Greenslade, D. J. M., Pattiaratchi, C., Badal, R., Synolakis,
880 C. E., and Kânoğlu, U. (2011). “A new tool for inundation modeling: Community Modeling

881 Interface for Tsunamis (ComMIT).” *Pure and Applied Geophysics*, 168(11), 2121–2131.

882 Titov, V. V. and Synolakis, C. E. (1995). “Modeling of breaking and nonbreaking long-
883 wave evolution and runup using VTCS-2.” *Journal of Waterway Port Coastal and Ocean*
884 *Engineering-ASCE*, 121, 308–316.

885 Titov, V. V. and Synolakis, C. E. (1998). “Numerical modeling of tidal wave runup.” *Journal*
886 *of Waterway Port Coastal and Ocean Engineering-ASCE*, 124(4), 157–171.

887 Uslu, B. (2008). “Deterministic and probabilistic tsunami studies in California from near and
888 farfield sources.” Ph.D. thesis, University of Southern California, Los Angeles, California
889 (August).

890 Uslu, B., Borrero, J. C., Dengler, L. A., and Synolakis, C. E. (2007). “Tsunami inundation at
891 Crescent City, California generated by earthquakes along the Cascadia Subduction Zone.”
892 *Geophysical Research Letters*, 34(20), L20601.

893 Uslu, B., Power, W., Greenslade, D., Eble, M., and Titov, V. (2011). “The July 15, 2009
894 Fiordland, New Zealand tsunami: Real-time assessment.” *Pure and Applied Geophysics*,
895 168(11), 1963–1972.

896 Valle, B. L., Kalligeris, N., Findikakis, A. N., Okal, E. A., and Synolakis, C. E. (2014).
897 “Plausible megathrust earthquakes in the eastern Mediterranean Sea.” *Engineering and*
898 *Computational Mechanics*, 167, 99–105.

899 Wei, Y., Bernard, E. N., Tang, L., Weiss, R., Titov, V. V., Moore, C., Spillane, M., Hopkins,
900 M., and Kânoğlu, U. (2008). “Real-time experimental forecast of the Peruvian tsunami of
901 August 2007 for US coastlines.” *Geophysical Research Letters*, 35(4), L04609.

902 Wei, Y., Chamberlin, C., Titov, V. V., Tang, L., and Bernard, E. N. (2013). “Modeling of
903 the 2011 Japan Tsunami: Lessons for near-field forecast.” *Pure and Applied Geophysics*,
904 170(6-8), 1309–1331.

905 Yeh, H., Liu, P. L.-F., Briggs, M., and Synolakis, C. (1994). “Propagation and amplification
906 of tsunamis at coastal boundaries.” *Nature*, 372(6504), 353–355.

907 H. Yeh, P. L.-F. Liu, and C. Synolakis, eds. (1996). *Long-wave runup models*. World Scientific

908 Publishing Co. Pte. Ltd., Singapore.

909 Zelt, J. A. (1991). “The run-up of nonbreaking and breaking solitary waves.” *Coastal Engi-*
910 *neering*, 15(3), 205–246.

911 Zhou, H., Wei, Y., and Titov, V. V. (2012). “Dispersive modeling of the 2009 Samoa
912 Tsunami.” *Geophysical Research Letters*, 39(16), L16603.

913 **List of Tables**

914 1 Representative forecast accuracies since 2004. 40

TABLE 1. Representative forecast accuracies since 2004.

Event number	Event Date	Event location	Earthquake magnitude, M_w	Number of forecasts	Model accuracy
1	26 December 2004	Sumatra	9.1	-*	Amplitudes bellow noise
2	3 May 2006	Tonga	7.9	8	70%
3	15 November 2006	Central Kuril Islands	8.3	12	85%
4	13 January 2007	Kuril Islands	8.1	15	78%
5	1 April 2007	Solomon Islands	8.1	7	Amplitudes bellow noise
6	15 August 2007	Peru	8.0	14	95%
7	12 September 2007	Sumatra	8.4	16	95%
8	14 November 2007	Antofagasts	7.7	4	Amplitudes bellow noise
9	15 January 2009	Kuril Islands	7.7	7	Amplitudes bellow noise
10	18 February 2009	Kermadec Islands	7.3	-*	Amplitudes bellow noise
11	19 March 2009	Kermadec Islands	7.8	6	Amplitudes bellow noise
12	10 August 2009	Andaman	7.7	-*	Amplitudes bellow noise
13	29 September 2009	Samoa	8.0	15	75%
14	3 January 2010	Solomon	7.2	-*	Amplitudes bellow noise
15	27 February 2010	Chile	8.8	25	76%
16	6 April 2010	Northern Sumatra	7.8	-*	Amplitudes bellow noise
17	25 October 2010	Mentawai, Indonesia	7.7	-*	Amplitudes bellow noise
18	21 December 2010	Bonin Islands	7.4	6	Amplitudes bellow noise
19	25 December 2010	Vanuatu	7.3	1	Amplitudes bellow noise
20	11 March 2011	Tohoku	9.1	32	69%
21	6 July 2011	Kermadec Islands	7.6	2	Amplitudes bellow noise
22	11 April 2012	Sumatra	8.6	-*	Amplitudes bellow noise
23	27 August 2012	El Saldova	7.4	-*	Amplitudes bellow noise
24	5 September 2012	Costa Rica	7.6	-*	Amplitudes bellow noise
25	28 October 2012	Haida Gwaii	7.8	38	68%
26	7 November 2012	Guatemala	7.4	-*	Amplitudes bellow noise
27	7 December 2012	Honshu, Japan	7.2	54	Amplitudes bellow noise
28	6 February 2013	Santa Cruz Islands	7.9	30	78%
29	1 April 2014	Iquique, Chile	8.1	31	85%
30	12 April 2014	Solomon Islands	7.6	3	Amplitudes bellow noise
31	13 April 2014	Solomon Islands	7.4	-*	Amplitudes bellow noise
32	18 April 2014	Guerrero, Mexico	7.3	-*	Amplitudes bellow noise
33	19 April 2014	Solomon Islands	7.5	-*	Amplitudes bellow noise
34	14 October 2014	Nicaragua	7.3	-*	Amplitudes bellow noise
35	18 July 2015	Santa Cruz Islands	6.9	-*	Amplitudes bellow noise
36	16 September 2015	Chile	8.3	38	71%
Summary			Range of M_w 7.2 - 9.1	Total forecasts 364	Average accuracy 79%

*Note: No high-resolution coastal forecast models were run. Only deep-water tsunami propagation forecast was performed based on DART data comparison.

915 **List of Figures**

916 1 MOST propagation model simulation of the 1996 Andreanov tsunami and
917 comparison with bottom pressure recordings, one of the first open ocean
918 records of a tsunami with a tsunameter. Red and blue lines represent buoy
919 measurements and model estimates respectively. 43

920 2 Current DART array of the International Tsunami Warning System. 44

921 3 Near-shore MOST estimates of the 2011 Tohoku tsunami flooding. Tsunami
922 flooding area at Sendai plain area shown for three forecast sources obtained
923 with (a) one-, (b) two- and (c) three-DART recordings (Kânoğlu et al. 2015). 45

924 4 Model forecast of flooding in Midway Atoll from the 2011 Tohoku tsunami.
925 Upper panel shows MOST results with blue-and-red colors showing the second
926 tsunami wave inundating the atoll lagoon (white arrow shows the direction of
927 tsunami propagation) including comparison of forecast wave height estimate
928 with tide gage measurement (inset). Green-yellow-red colors over the islands
929 show maximum forecasted inundation. Bottom panel shows flooding area
930 measured after the event. 46

931 5 MOST results for the 2011 Tohoku tsunami impact at Crescent City, Califor-
932 nia. Left panel shows tide gage model (red line) and measurement including
933 tidal level change (black line) during the event. The location of the tide gage
934 is shown as black triangle on the map. Right panel shows results of the same
935 event simulation done at high tide level and associated flooding on Tweb map. 47

936	6	Tsunami events since 2004 used in real-time benchmarking of MOST flood-	
937		ing forecast. The mosaic of maximum offshore amplitudes computed with	
938		MOST model are shown as representation of tsunami energy distribution dur-	
939		ing ocean-wide propagation. The tsunamis are listed in Table 1 and are given	
940		in chronological order left to right, top to down, starting from the 2004 Indian	
941		Ocean on top left, ending at 2015 Chilean tsunami on lower right. Thirty-six	
942		events shown in the figure are the tsunamis recorded at DARTs (except the	
943		Indian Ocean tsunami), the data that constrained the real-time assessment	
944		with the MOST model.	48

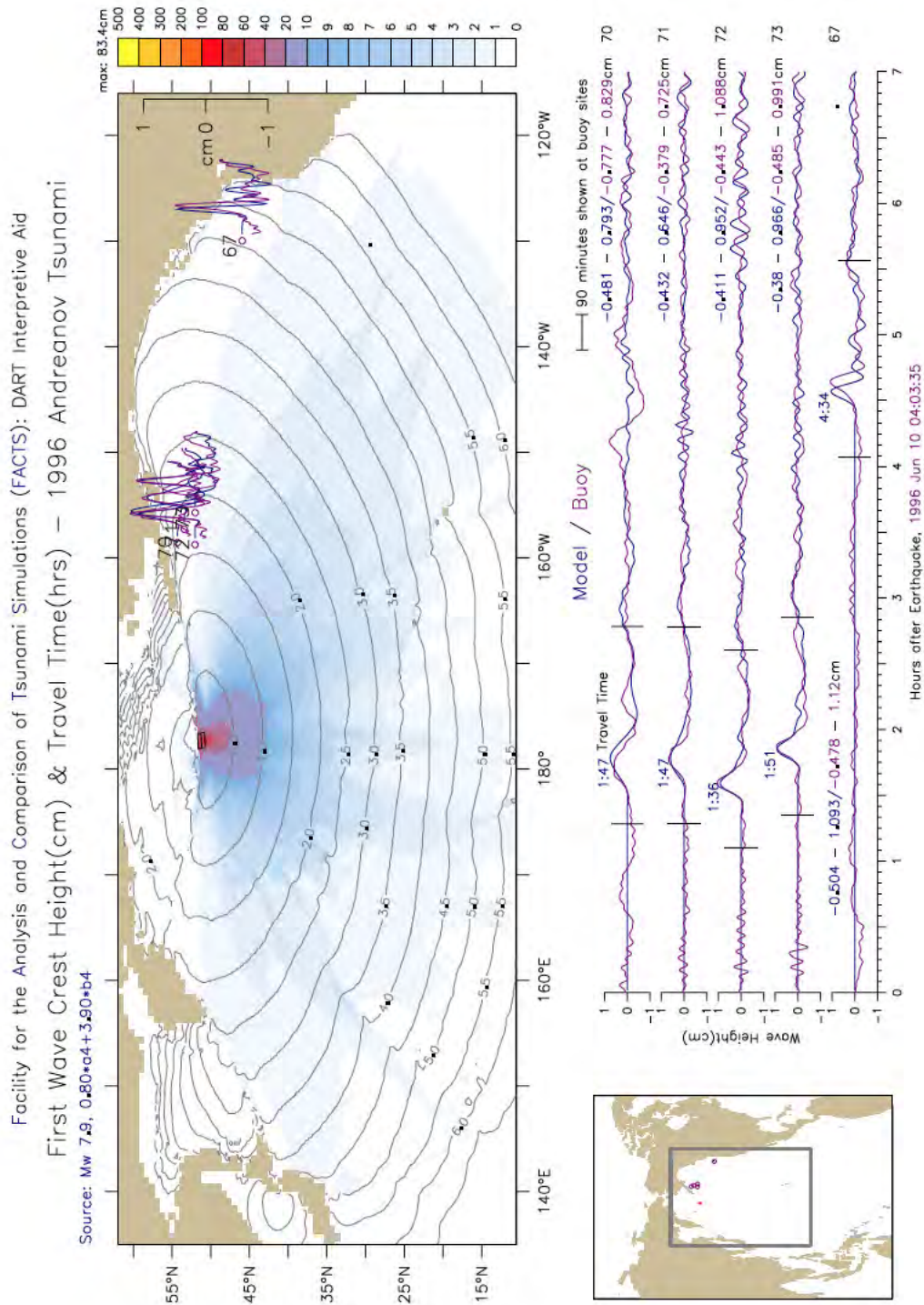


FIG. 1. MOST propagation model simulation of the 1996 Andreanov tsunami and comparison with bottom pressure recordings, one of the first open ocean records of a tsunami with a tsunameter. Red and blue lines represent buoy measurements and model estimates respectively.

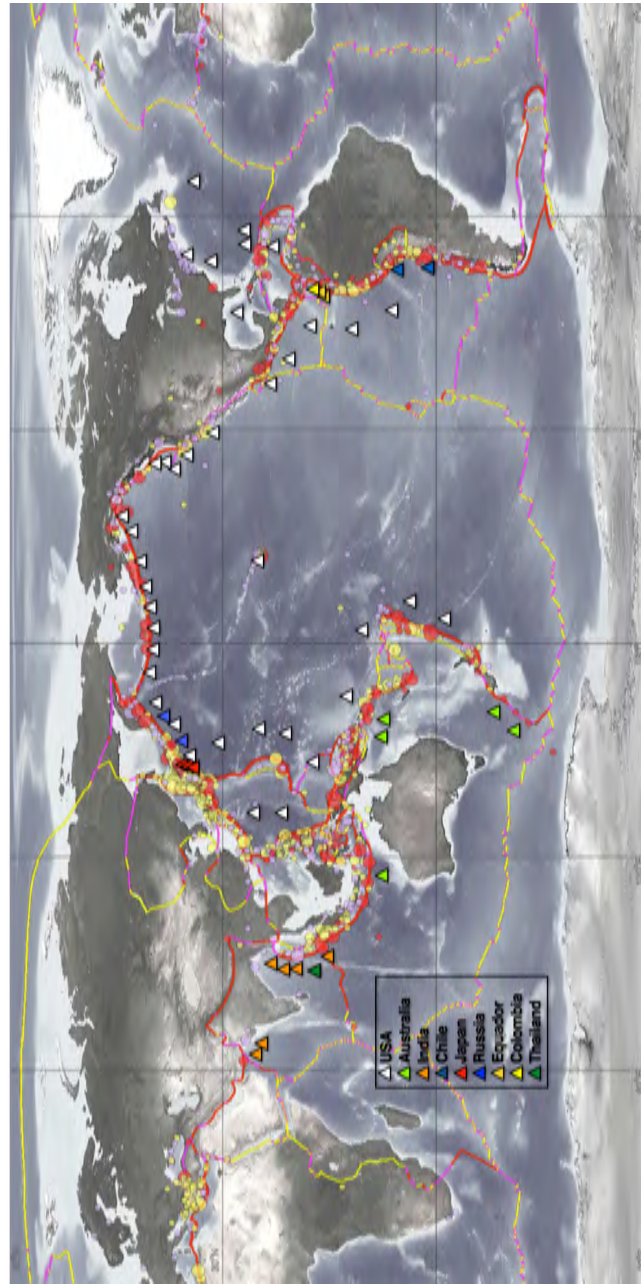


FIG. 2. Current DART array of the International Tsunami Warning System.

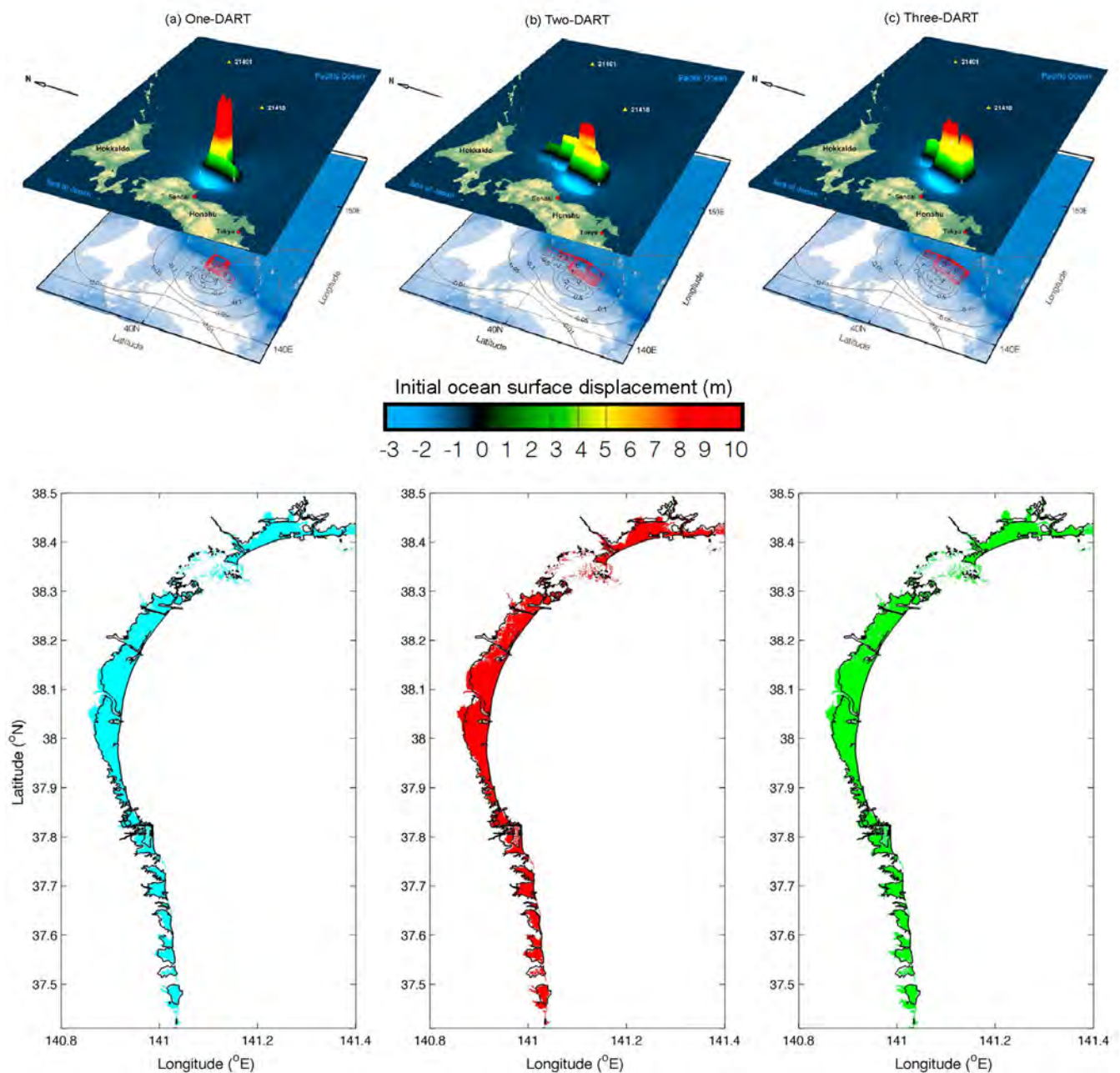


FIG. 3. Near-shore MOST estimates of the 2011 Tohoku tsunami flooding. Tsunami flooding area at Sendai plain area shown for three forecast sources obtained with (a) one-, (b) two- and (c) three-DART recordings (Kânoğlu et al. 2015).

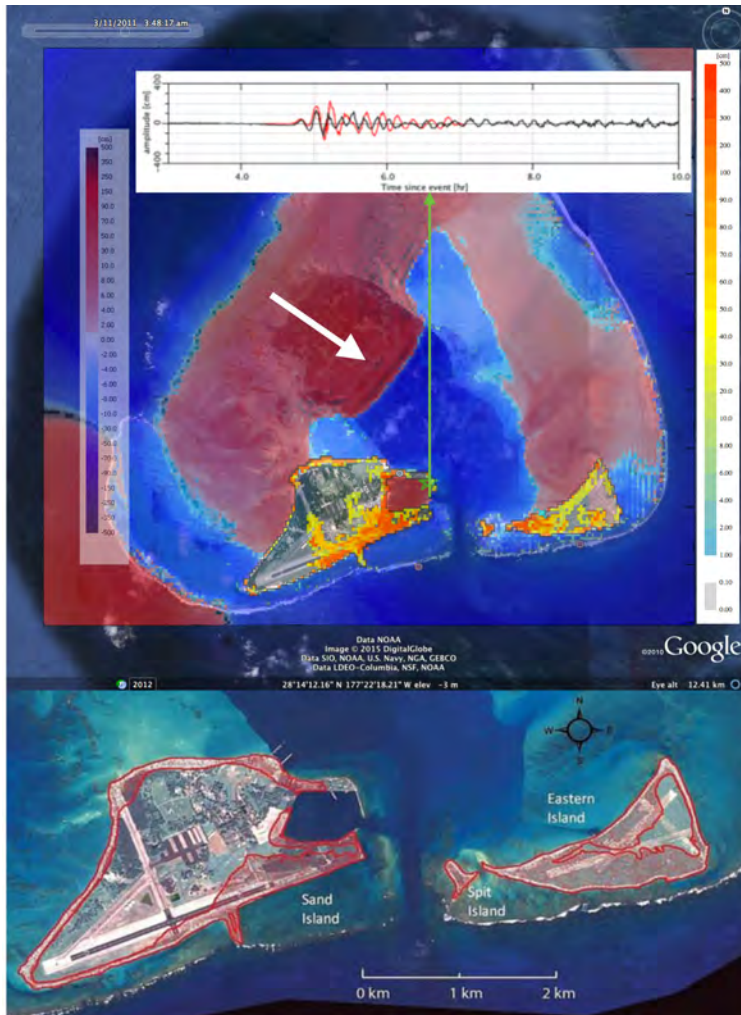


FIG. 4. Model forecast of flooding in Midway Atoll from the 2011 Tohoku tsunami. Upper panel shows MOST results with blue-and-red colors showing the second tsunami wave inundating the atoll lagoon (white arrow shows the direction of tsunami propagation) including comparison of forecast wave height estimate with tide gage measurement (inset). Green-yellow-red colors over the islands show maximum forecasted inundation. Bottom panel shows flooding area measured after the event.

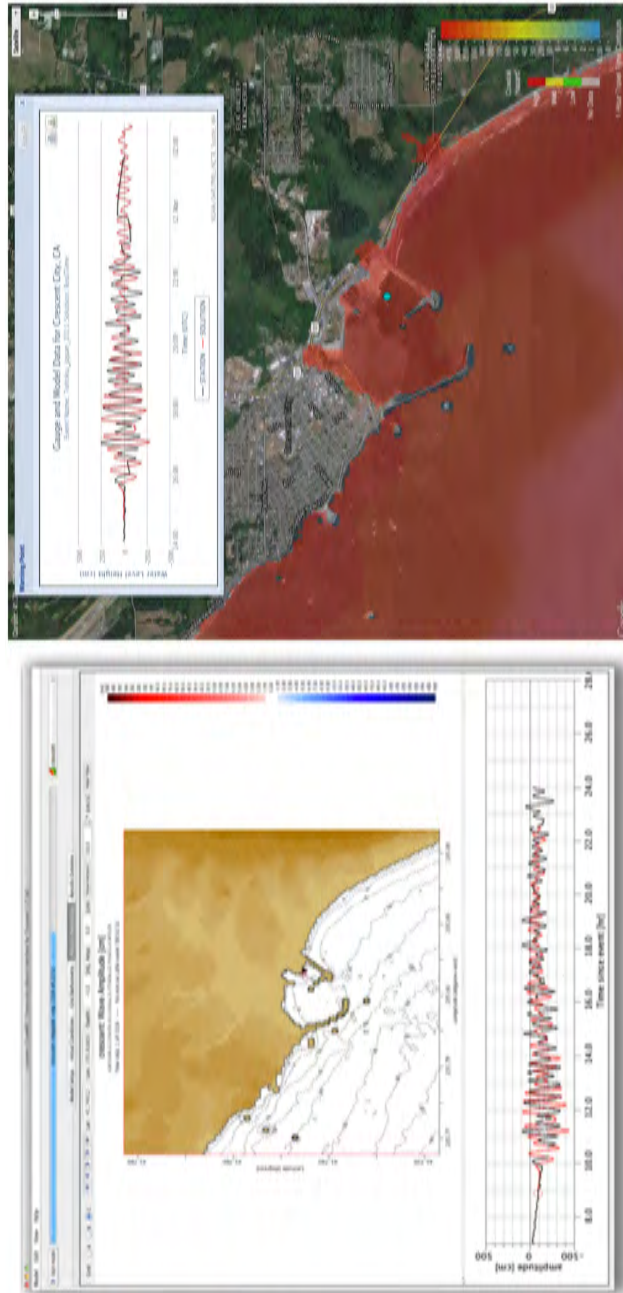


FIG. 5. MOST results for the 2011 Tohoku tsunami impact at Crescent City, California. Left panel shows tide gage model (red line) and measurement including tidal level change (black line) during the event. The location of the tide gage is shown as black triangle on the map. Right panel shows results of the same event simulation done at high tide level and associated flooding on Tweb map.

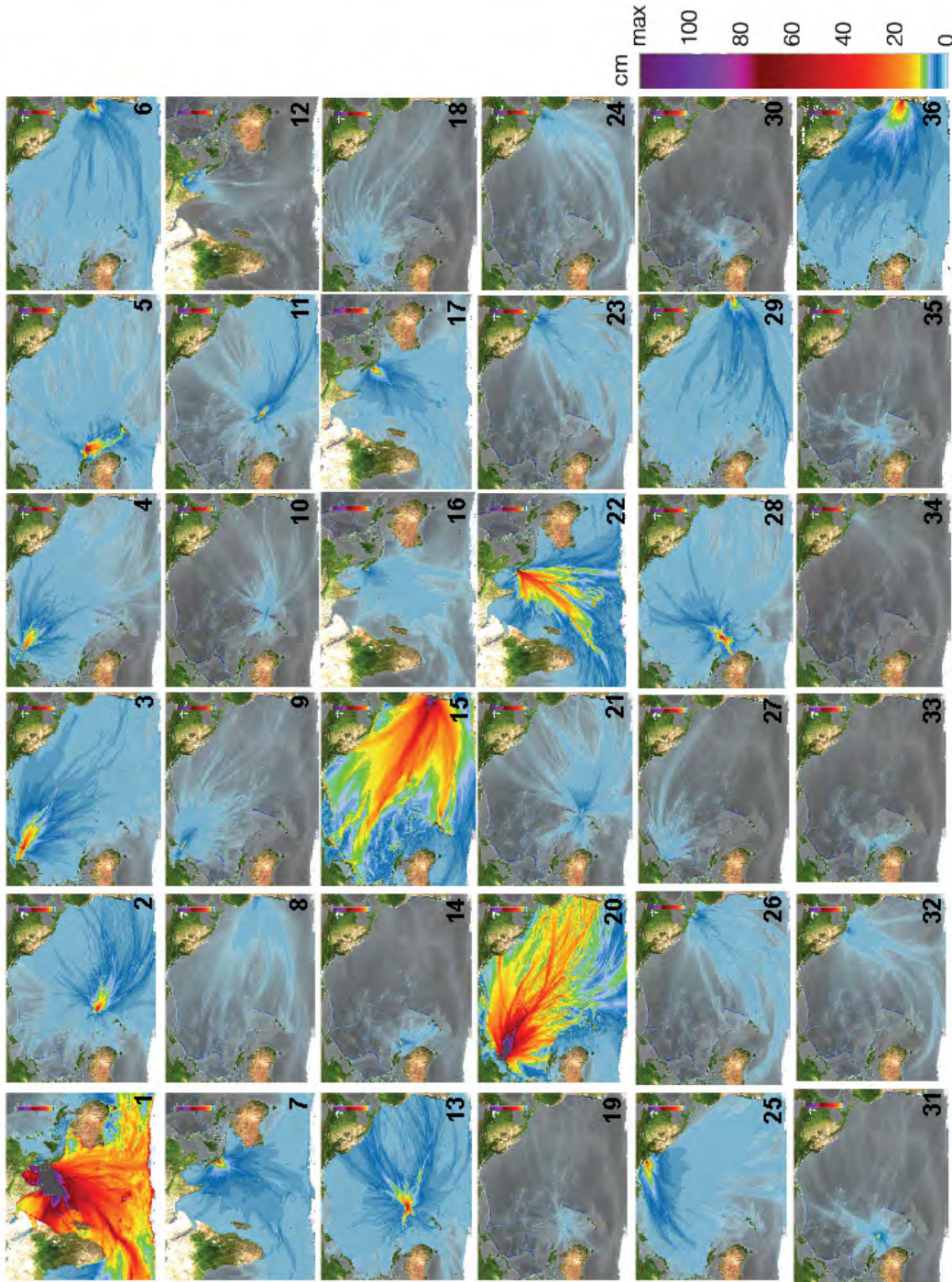


FIG. 6. Tsunami events since 2004 used in real-time benchmarking of MOST flooding forecast. The mosaic of maximum offshore amplitudes computed with MOST model are shown as representation of tsunami energy distribution during ocean-wide propagation. The tsunamis are listed in Table 1 and are given in chronological order left to right, top to down, starting from the 2004 Indian Ocean on top left, ending at 2015 Chilean tsunami on lower right. Thirty-six events shown in the figure are the tsunamis recorded at DARTs (except the Indian Ocean tsunami), the data that constrained the real-time assessment with the MOST model.